12-2016

Analytical Modeling and Numerical Simulation of a Thermoelectric Generator Including Contact Resistances

Shripad Dhoopagunta
Western Michigan University, shripad.dhoopagunta@gmail.com

ANALYTICAL MODELING AND NUMERICAL SIMULATION OF A THERMOELECTRIC GENERATOR INCLUDING CONTACT RESISTANCES

by

Shripad Dhoopagunta

A thesis submitted to the Graduate College
in partial fulfillment of the requirements
for the degree of Master of Science in Engineering (Mechanical)
Mechanical and Aerospace Engineering
Western Michigan University
December 2016

Thesis Committee:

HoSung Lee, Ph.D., Chair
Bade Shreshta, Ph.D.
Chris Cho, Ph.D.

ANALYTICAL MODELING AND NUMERICAL SIMULATION OF A THERMOELECTRIC GENERATOR INCLUDING CONTACT RESISTANCES

Shripad Dhoopagunta, M.S.E.

Western Michigan University, 2016

With increasing demand for energy harvesting systems, research has been conducted in different areas in which Thermoelectric Generators (TEG) find their way into the top of many available resources. Out of many energy harvesting systems available, TEGs are comparatively easier to study, to manufacture and also to comprehend while producing enough energy for applications they find use in. They are solid state devices, meaning; they do not have any moving parts and hence makes them durable. Most of the energy that goes out of the automobile as exhaust is reused to power the TEGs. In most of the works that's been analyzed, only electrical impedence matching was considered while thermal impedence matching including heat exchangers was ignored. This project explores the possibility of obtaining higher power output while both these matchings were simultaneously considered. An ideal and effective way of generating power will be discussed, which is established by optimizing a thermoelectric module. A one dimensional analytical model is developed in Mathcad. Later, a 3D model of the same has been numerically simulated using ANSYS workbench. Insights of the numerical modelling has been discussed and the results show that the Power Output of a TEG can be drastically improved at low leg lengths. The electrical resistance of the contact material and also the copper conductor cannot be neglected. Also the thermal conductance of the ceramic substrates can be changed by changing its material to Aluminum Nitride (AIN) which makes the power output close to an ideal case.

ACKNOWLEDGEMENTS

I would like to thank my advisor Dr. HoSung Lee for his encouragement for my work. This work would not have been possible without his support and guidance. It has been a pleasure working with him and learning everything he has taught us.

I would also like to extend my thanks to my committee members, Dr. Bade Shreshta and Dr. Chris Cho, for their guidance and suggestions to improve the quality of this work.

I would also like to thank my family, my mother, my father, and my brother for their support and trust they had placed in me. Their belief in me is a big part of my accomplishment.

Last but not the least, I would like to thank my friends who believed in me and supported me throughout my work with this project.

Shripad Dhoopagunta

TABLE OF CONTENTS

Table of Contents - Continued

LIST OF TABLES

LIST OF FIGURES

List of Figures - Continued

NOMENCLATURE

A_c	total fin surface area cold side heat sink (mm^2)
A_e	cross-sectional area of thermo element (mm^2)
A_h	total fin surface area hot side heat sink (mm^2)
A_M	base area of thermoelectric module (mm^2)
COP	the coefficient of performance
c_p	specific heat (J/kg.K)
G_e	thermocouple geometric ratio
H	total height of thermoelectric air conditioner (mm)
h	heat transfer coefficient of the fluid (W/m^2K)
I	electric current (A)
j	unit cell number
k	thermoelement thermal conductivity (W/m K), $k = k_p + k_n$
K	thermal conductance (W/K), $K = kA_e/L_e$
L_e	length of thermoelement or thermoelectric leg (mm)
n	the number of thermocouples
N_k	dimensionless thermal conductance, $N_k = n(A_e k/L_e)/\eta_h h_h A_h$
N_h	dimensionless convection, $N_h = \eta_c h_c A_c/\eta_h h_h A_h$
N_I	dimensionless current, $N_I = \alpha I/(A_e k/L_e)$
P_{in}	input power (W)

q_x the rate of heat transfer around the differential element

$\dot{Q}$ the rate of heat transfer

$\dot{Q}_c$ cooling capacity (W)

$\dot{Q}_h$ heat rejection (W)

R_{Al} thermal resistance of the aluminum block

t_{al} thickness of the aluminum block

T_c cold junction temperature (°C)

T_h hot junction temperature (°C)

$T_{\infty c}$ cold fluid temperature (°C)

$T_{\infty h}$ hot fluid temperature (°C)

$\dot{V}_c$ cold fluid volume flow rate (CFM)

$\dot{V}_h$ hot fluid volume flow rate (CFM)

W total width of thermoelectric air conditioner (mm)

$\dot{W}$ electrical power (W)

x direction along the length of the element

Z the figure of merit (1/K) $= \alpha^2/\rho k$

Greek symbols

α Seebeck coefficient (V/K), $\alpha = \alpha_p - \alpha_n$

ρ electrical resistivity (Ω cm), $\rho = \rho_p + \rho_n$

φ alimunum block thermal resistance (K/W)

η fin efficiency of the heat sink

γ thermal resistances ratio between the heat sink and aluminum block

Subscripts

al aluminum

c cold

ct contact

e thermoelement

h hot

in inlet

j unit cell number

m measured

n n-type element

no the number of thermocouples

out outlet

opt. optimal quantity

p p-type element

$*$ dimensionless

∞ fluid

1 INTRODUCTION

Thermoelectric (TE) devices, the name itself sates that it is a device which involves thermal and an electrical energy. These devices either produce electricity when heat is supplied also known as TE generators (TEG) or produce heat or cooling effect when electricity is supplied called TE coolers (TEC). Thermoelectric devices are solid state devices, meaning they don't have any moving parts which is why they find their way in a lot of applications. These devices have the potential to replace the traditional air conditioners and HVAC systems in a motor vehicle if properly optimized.

1.1 Physics of Thermoelectrics

Thermoelectrics is encompassed around three physics, the Seebeck Effect, Thomson Effect and the Peltier effect.

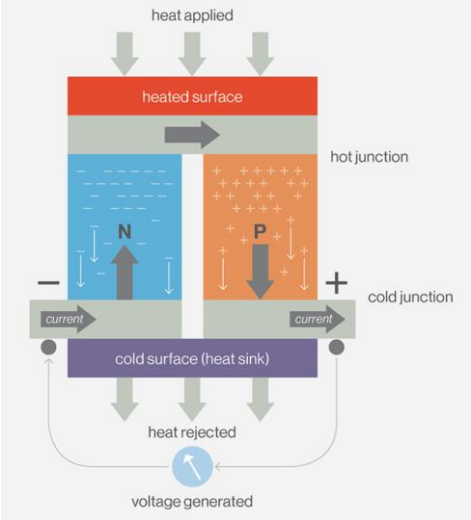

Figure 1-1 Thermoelectric effect

1.1.1 Seebeck effect

In the early 19th century, Thomas J. Seebeck discovered that when a circuit is made of two dissimilar materials then an electro motive force can be produced by creating a temperature difference between the junctions of the materials. This effect is called the Seebeck Effect.

$$V = \alpha \Delta T \tag{1.1}$$

In equation 1.1), 'V' is the electric potential produced by the temperature difference ΔT. α is the proportionality constant that relates the electric potential and the temperature difference called the Seebeck coefficient. In most of the material Seebeck Coefficient is a function of temperature but for studies to be simple people consider it a constant value.

1.1.2 Peltier effect

The exact opposite effect of Seebeck is the Peltier effect. This states that when a current is supplied to two dissimilar materials connect in a closed circuit heat is either rejected or absorbed at the junctions. This effect has been discovered by Jean Peltier in the mid-19th century.

$$Q_{peltier} = \Pi_{AB} I \tag{1.2}$$

Here, Π_{AB} is the Peltier coefficient, $Q_{peltier}$ is the total heat added or rejected by the system and I is the current passing through the thermoelectric element.

1.1.3 Thomson effect

In 1854, William Thomson, discovered that when a current is passed in a conductor there is temperature difference that exists in it which depends on the direction of the current in the circuit. This is similar to Peltier effect, but he precisely says that all the thermoelectric effects combine each other. The Thosmson effect is given by the following equation

$$Q_{Thomson}=\tau I \Delta T \quad (1.3)$$

τ is the Thomson Coefficient in the above equation.

1.2 Figure of Merit

The figure of merit is a simple and an easy form of representing the efficiency of the model. It is depicts the performance of the Thermoelectric module. It is represented by the letter Z which has the units of '1/K'. It is given by the

$$Z = \frac{\alpha^2}{\rho k} = \frac{\alpha^2 \sigma}{k} \quad (1.4)$$

Where 'α' is the Seebeck coefficient, 'k' is the thermal conductivity and 'ρ' is the electrical conductivity of the materials. '$\alpha^2 \sigma$' is called the power factor in which $\sigma = 1/\rho$ is the electrical conductivity.

Z becomes a unit less quantity when multiplied by temperature 'T' and this number is used as a standard of the material in the TE industry. The term ZT is called the dimensionless figure of merit. The more the ZT value the better the device performs in producing electricity. To increase ZT the power factor has to be increased and also the 'k' thermal conductivity of the material has to decrease. This all depends on the material and hence improving the figure of merit is related to material science. The most common material used in Thermoelectrics is the Bismuth Telluride which has ZT = 1 at room temperature.

With the increase in Nano technology developments in the recent days the figure of merit of different material has been improved. Other material like the Lead Telluride and the Silicon Germanium have a higher ZT value at higher temperatures. This can be seen in the following graph

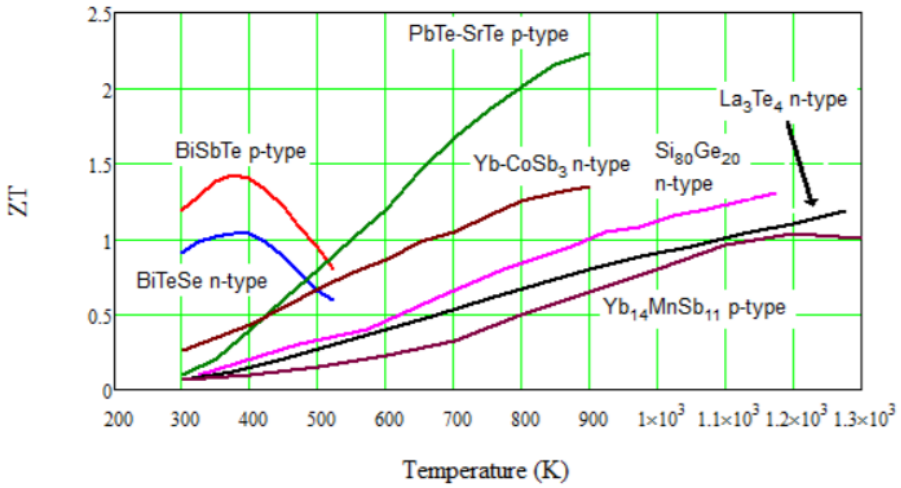

Figure 1-2 Dimensionless figure of merit

1.3 The Thermoelectric Module

A p-type semiconductor and an n-type semiconductor connected electrically in series and thermally in parallel to produce electricity or heat through the Seebeck and the Peltier effects is called a thermoelectric couple. Number of such p-type and n-type semiconductor devices when connected form a thermoelectric module. The modules always has a ceramic substrate on the top and bottom as shown in the Figure 1-3 which acts as an electric insulator.

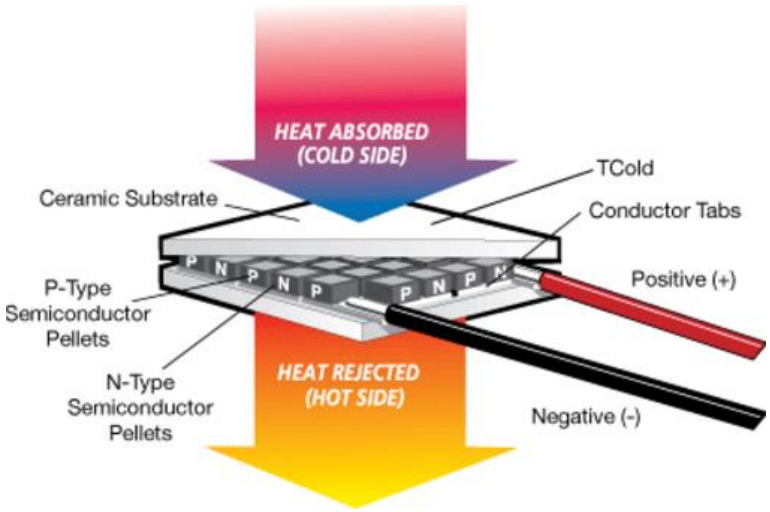

Figure 1-3 Thermoelectric module

1.4 Thermoelectric System

A thermoelectric system generates power using a number or thermoelectric modules. To do this there should be a lot of temperature difference on either sides of the Thermoelectric Generator (TEG). These systems find their application in producing power from an exhaust gas of an automobile engine. The exhaust is treated as the hot side and the cold side is cooled by coolants of the engine. The System uses heat exchangers to increase the amount of heat that enters the TE module. Optimizing the heat exchanges id a very difficult task in such systems. Balancing the heat and producing more electric power which leads to better efficiency is a challenging mission for the TEG industry.

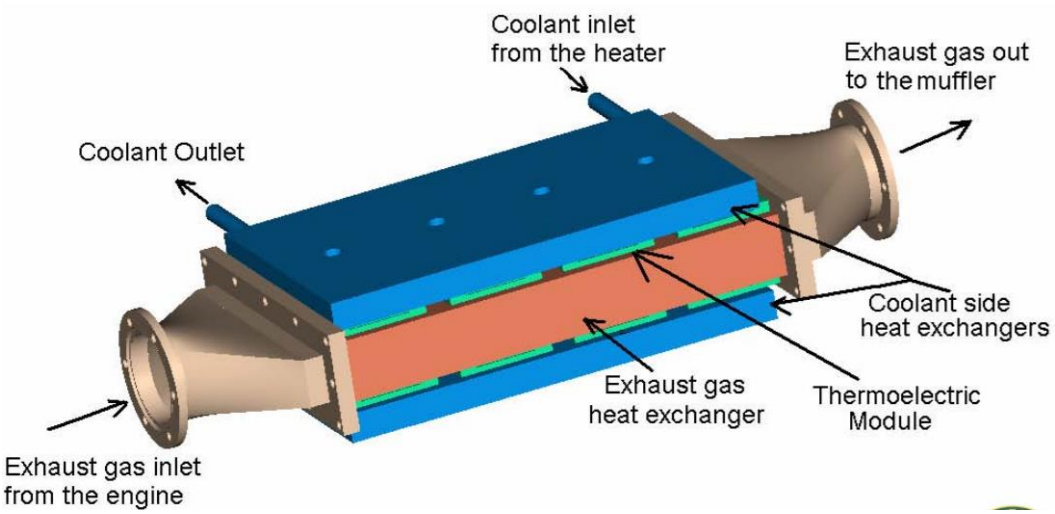

Figure 1-4 Thermoelectric generator system

1.5 Governing Equations of Thermoelectrics

As mentioned in 1.1 the governing equations of thermoelectric revolve around the three effects, the Seebeck effect, Thomson effect and the Peltier Effect. The differential form of the governing equations can be derived as follows.

Considering a non-uniformly heated thermoelectric material for isotropic material properties, the continuity equation is given as

$$\vec{\nabla} \cdot \vec{j} = 0 \qquad 1.5$$

Where $\vec{\nabla}$ is the differential operator along with respect to length and $\vec{j}$ is the current density. The electric field $\vec{E}$ is affected by $\vec{j}$ and the temperature gradient $\vec{\nabla}T$. The coefficients have contributions from both Ohm's law and the Seebeck effect. By differentiating Eq.1.5 with respect to length, the electric field is equal to

$$\vec{E} = \vec{j}\,\rho + \alpha\,\vec{\nabla}T \qquad 1.6$$

The heat flow density vector (heat flux) is given by

$$\vec{q} = \alpha T \vec{j} - k \vec{\nabla} T \tag{1.7}$$

The general heat diffusion equation is expressed as

$$-\vec{\nabla} \cdot \vec{q} + \dot{q} = \rho c_p \frac{\partial T}{\partial t} \tag{1.8}$$

where $\dot{q}$ is the generated heat by unit volume, ρ is the mass density, c_p is the specific heat and $\frac{\partial T}{\partial t}$ is the rate of change temperature with respect to time.

For steady state Eq. 1.7 reduced to

$$-\vec{\nabla} \cdot \vec{q} + \dot{q} = 0 \tag{1.9}$$

where $\dot{q}$ is defined as

$$\dot{q} = \vec{E} \cdot \vec{j} = J^2 \rho + \vec{j} \cdot \alpha \vec{\nabla} T \tag{1.10}$$

Finally by substituting the eqs 1.7, 1.91.10 into 1.9 we get

$$\vec{\nabla} \cdot \left(k \vec{\nabla} T\right) + J^2 \rho - T \frac{d\alpha}{dT} \vec{j} \cdot \vec{\nabla} T = 0 \tag{1.11}$$

where $\vec{\nabla} \cdot \left(k \vec{\nabla} T\right)$ is the thermal conduction, $J^2 \rho$ is the Joule heating, and $T \frac{d\alpha}{dT}$ is the Thomson coefficient. A study by [1] shows a good agreement between the Thomson coefficient as a function of temperature and the exact solution that neglected the Thomson coefficient. Hence, the Thomson coefficient can be neglected $T \frac{d\alpha}{dT} = 0$.

2 THERMOELECTRICS AND ITS APPLICATIONS

Thermoelectric devices are steady state devices which means they have no moving parts and hence they find their use in a lot of applications. TEGs are mostly used where there is lot of temperature difference and energy being wasted, while TECs are used where there is low temperature difference and cooling is need. Peltier models have also been used in many everyday life situations like cool storage boxes for medicine or for cooling boxes for picnic storage [2].

Small devices like the safety surveillance, remote control etc. mostly rely on batteries which have a lot of disadvantages. Batteries have a limited power supply and have to be replaced and also have chemical energy which is harmful to the environment. An alternate solution for these batteries are the solar cells but if there is no light then these are of no use. Hence thermoelectric generators are gaining importance in replacing such systems. They can generate enough power for a very small temperature difference. [3]

In recent studies, it has been found that thermoelectrics are useful in applications where the supply of heat is cheap or free or is being wasted. One of the few disadvantages that these devices have is that the efficiency is very low when the power generation is maximum. Hence, they need an unlimited source of energy. The use of such waste heat is exploited by thermoelectrics and is found in places like the exhaust of an automobile where the energy generated by the TEs is enough to run the electronics. [4]

The concept of thermoelectrics can also use solar energy. The thermal energy from the sun has enough temperature difference to power TE generators. The temperature difference that they produce with highly sophisticated solar concentrators is about 1200 K. At that temperature

difference the efficiency of the TE generators is very low. Research is being conducted to improve the efficiency and also the power output from such systems. This kind of energy produced will serve as a reliable source of energy.

Apart from all the above applications thermoelectrics are also used in sensors in the medical field. They are used as cryogenic heat flux sensors [5], ultrasonic intensity sensors [6], thin film sensors (measure very small dimension) [7], and infrared sensors and also as fluid sensors (measure velocity of the fluid) [8].

Some of the most recent applications in the concept of thermoelectric cooling is in vehicle air conditioning. Almost 10% of the annual consumption of fuel can be directed to the use of air conditioning [9]. Most of these use refrigerants like R-134a which has adverse effects on the environment being a major greenhouse gas. There is a lot of debate in the current day about banning all the environment depleting compounds and R-134a is definitely one of them. [10]. The U.S. Department of Energy (DOE) and the California Energy Commission funded a project to research an application involving thermoelectric heat ventilating and air conditioning system (TE HVAC) that promised to replace the traditional air conditioning systems in vehicles [9] [11]. Use of a thermoelectric air conditioning system (TEAC) in place of the traditional air conditioning system has been proven to have benefits such as being able to produce a cooling effect without the use of environment depleting substance like the R-134 and also having a scope to select the areas needing heating or cooling instead of randomly cooling the whole area which in turn reduces the amount of fuel consumed considerably hence also reducing the exhaust [9].

2.1 Thermoelectrics Today

Although the concept of thermoelectrics was observed centuries ago, the first model of its kind had come out only in the recent times. The first ever functioning device was developed in the late 1950s. These are also known as the first generation thermoelectric devices. After a lot of questioning, answering and debating, many theories had been developed on various genres of this concept. Some of them included the study of thermoelectric properties with reduction in size. Early 90s saw the rise of experimental research that eventually gave several advances in the early 21st century.

Nano material have been discovered to have an effect on the value of the figure of merit that is worth noting. Due to an inverse relation between all the three parameters linking the figure of merit, it becomes more difficult to model a device that agrees to produce a higher value of ZT. Hence, the lattice thermal conductivity of the material was taken advantage of because this is the only parameter that seems independent of the electronic structure of the model.

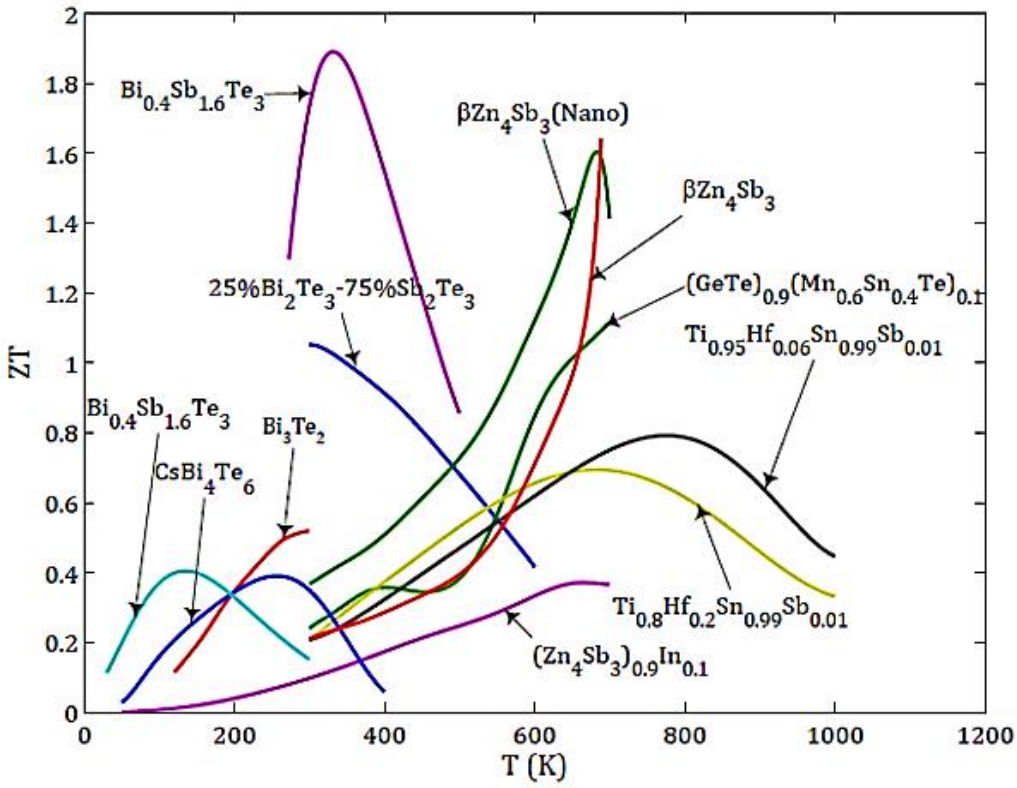

Figure 2-1 Dimensionless figure of merit vs. temperature

2.2 Thermoelectric Ideal (standard) Equations

2.2.1 General governing equations

Considering a non-uniformly heated thermoelectric material for isotropic material properties, the continuity equation is given as

$$\vec{\nabla} \cdot \vec{j} = 0 \qquad 2.1$$

Where $\vec{\nabla}$ is the differential operator along with respect to length and $\vec{j}$ is the current density. The electric field $\vec{E}$ is affected by $\vec{j}$ and the temperature gradient $\vec{\nabla}T$. The coefficients have

contributions from both Ohm's law and the Seebeck effect. By differentiating Eq. (2.1) With respect to length, the electric field is equal to

$$\vec{E} = \vec{j}\,\rho + \alpha\,\vec{\nabla}T \tag{2.2}$$

The heat flow density vector (heat flux) is given by

$$\vec{q} = \alpha\,T\,\vec{j} - k\,\vec{\nabla}\,T \tag{2.3}$$

The general heat diffusion equation is expressed as

$$-\vec{\nabla}\cdot\vec{q} + \dot{q} = \rho c_p\,\frac{\partial T}{\partial t} \tag{2.4}$$

Here, $\dot{q}$ is the generated heat by unit volume, ρ is the mass density, c_p is the specific heat and $\frac{\partial T}{\partial t}$ is the rate of change temperature with respect to time.

For steady state Eq. (2.3) reduced to

$$-\vec{\nabla}\cdot\vec{q} + \dot{q} = 0 \tag{2.5}$$

Where $\dot{q}$ is defined as

$$\dot{q} = \vec{E}\cdot\vec{j} = J^2\rho + \vec{j}\cdot\alpha\vec{\nabla}T \tag{2.6}$$

Following equation can be obtained by substituting Eqns. (2.3) and (2.6) in equation (2.5).

$$\vec{\nabla}\cdot\left(k\vec{\nabla}T\right) + J^2\rho - T\frac{d\alpha}{dT}\vec{j}\cdot\vec{\nabla}T = 0 \tag{2.7}$$

Where $\vec{\nabla} \cdot (k\vec{\nabla}T)$ is the thermal conduction, $J^2\rho$ is the Joule heating, and $T\frac{d\alpha}{dT}$ is the Thomson coefficient. A study by [12] shows a good agreement between the Thomson coefficient as a function of temperature and the exact solution that neglected the Thomson coefficient. Hence, the Thomson coefficient can be neglected $T\frac{d\alpha}{dT} = 0$.

Assumptions of thermoelectric ideal (standard) equations

Below are the important assumptions of thermoelectric ideal (standard) equations:

1) The Thomson effect is negligible. It has been proven analytically and experimentally that the Thomson effect has a very small effect on the performance of TEG and TEC.
2) The electrical and thermal resistances between ceramic plates and thermoelectric elements are negligible.
3) The convection and radiation losses are negligible.
4) The materials properties are assumed to be independent of temperature.

2.2.2 Thermoelectric couple equations

Consider two dissimilar semiconductor elements, which are sandwiched between copper conductive tabs, each element is called a thermoelectric leg or pellet, and is either p-type material (positive) or n-type material (negative). These elements are temperature independent with their material properties, which are Seebeck coefficient (α),electrical resistivity (ρ), and thermal conductivity (k), as illustrated in Figure 2-2

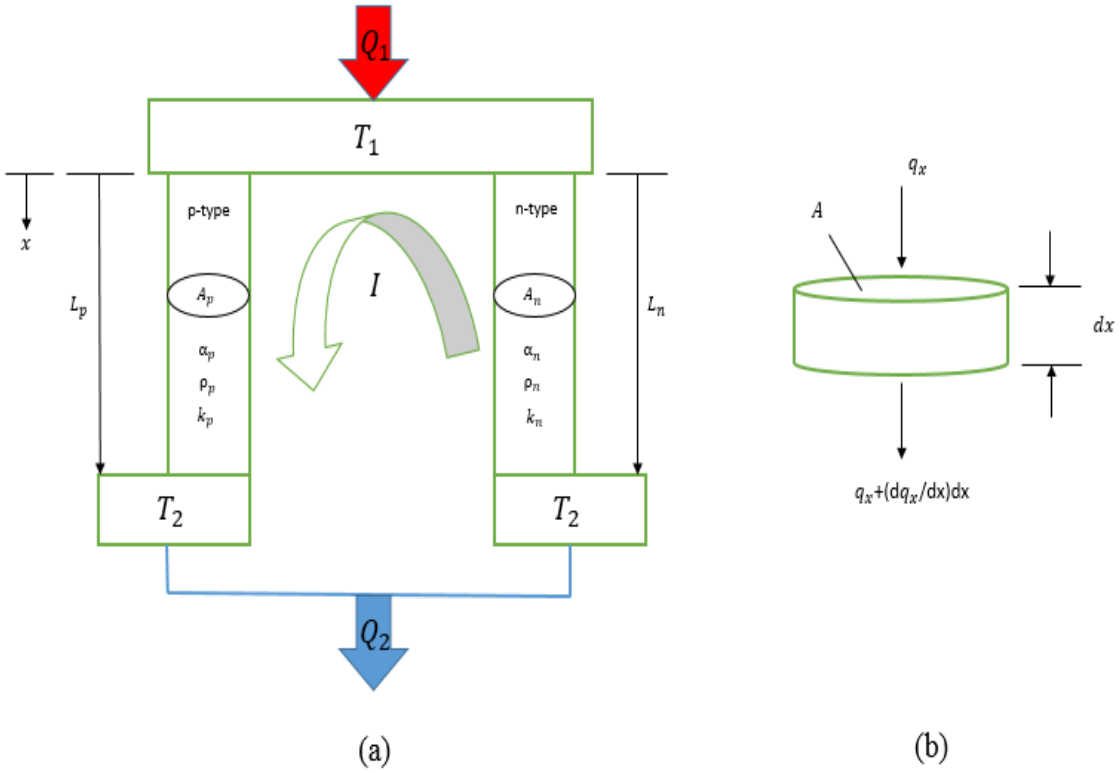

Figure 2-2 Longitudinal cross-section of a thermoelectric couple and differential element

The steady state heat balance at T_1 becomes

$$\dot{Q}_1 = q_p + q_n \tag{2.8}$$

where q_p and q_n are the heat flows for p-type and n-type. The heat flows can be defined in terms of the Peltier heat and Fourier's law of conduction as

$$q_n = -\alpha_n T_1 I + \left(-k_n A_n \left.\frac{dT}{dx}\right|_{x=0}\right) \tag{2.9}$$

$$q_p = \alpha_p T_1 I + \left(-k_p A_p \left.\frac{dT}{dx}\right|_{x=0}\right) \tag{2.10}$$

By applying the heat balance on the differential element shown in Figure 2-2, the temperature gradient can be obtained as

$$\underbrace{q_x - \left(q_x + \frac{dq_x}{dx}\right)}_{\substack{\text{heat transfer} \\ \text{across the surface} \\ \text{of the element}}} dx + \underbrace{\frac{I^2 \rho_p}{A_p} dx}_{\text{Joul heating}} = 0 \qquad 2.11$$

Differentiating Eq (2.10) with respect to x gives

$$\frac{dq_p}{dx} = -k_p A_p \frac{d}{dx}\left(\frac{dT}{dx}\right) \qquad 2.12$$

Inserting Eq. (2.12) into Eq. 2.11 yields

$$-\frac{d}{dx}\left(-k_p A_p \frac{dT}{dx}\right) + \frac{I^2 \rho_p}{A_p} = 0 \qquad 2.13$$

or,

$$k_p A_p \frac{d}{dx}\left(\frac{dT}{dx}\right) = \frac{-I^2 \rho}{A_p} \qquad 2.14$$

Integrating Eq. 2.14 gives

$$k_p A_p \int d\left(\frac{dT}{dx}\right) = -\frac{I^2 \rho}{A_p} \int dx \rightarrow \frac{dT}{dx} = -\frac{I^2 \rho}{k_p A_p^2} x + C_1 \qquad 2.15$$

Using the boundary conditions as T_1 at $x = 0$ and T_2 at $x = L$, Eq. 2.15 can be integrated from 0 to L and leads to

$$\int_{T_1}^{T_2} dT = -\frac{I^2\rho}{k_p A_p^2}\int_0^L x + \int_0^L x\, C_1 \rightarrow (T_2 - T_1) = -\frac{I^2\rho}{2k_p A_p^2}L^2 + C_1 L_p \qquad 2.16$$

From the above equation, C_1 can be obtained as

$$C_1 = \frac{I^2\rho}{2k_p A_p^2}L_p + \left(\frac{T_2 - T_1}{L_p}\right) \qquad 2.17$$

Substituting Eq.2.17 into Eq.2.15 at $x = 0$ gives

$$\left.\frac{dT}{dx}\right|_{x=0} = -\frac{I^2\rho}{2k_p A_p^2}L_p - \frac{(T_1 - T_2)}{L_p} \qquad 2.18$$

Substituting Eq. 2.18 into Eq. 2.10 yields

$$q_p = \alpha_p T_1 I - \frac{1}{2}I^2\frac{\rho_p L_p}{A_p} + \frac{k_p A_p}{L_p}(T_1 - T_2) \qquad 2.19$$

Eq. 2.19 represents the heat transfer for the p-type, by following the similar way the heat transfer equation for n-type can be derived as

$$q_n = -\alpha_n T_1 I - \frac{1}{2}I^2\frac{\rho_n L_n}{A_n} + \frac{k_n A_n}{L_n}(T_1 - T_2) \qquad 2.20$$

As shown in Eq.2.8, the heat transfer rates of thermoelectric couple equal to

$$\dot{Q}_1 = (\alpha_p - \alpha_n)T_1 I - \frac{1}{2}I^2\left(\frac{\rho_p L_p}{A_p} + \frac{\rho_n L_n}{A_n}\right) + \left(\frac{k_p A_p}{L_p} + \frac{k_n A_n}{L_n}\right)(T_1 - T_2) \quad 2.21$$

and,

$$\dot{Q}_2 = (\alpha_p - \alpha_n)T_2 I + \frac{1}{2}I^2\left(\frac{\rho_p L_p}{A_p} + \frac{\rho_n L_n}{A_n}\right) + \left(\frac{k_p A_p}{L_p} + \frac{k_n A_n}{L_n}\right)(T_1 - T_2) \quad 2.22$$

Moreover, the material properties can be added together using the following equations

$$\alpha = \alpha_p - \alpha_n \quad 2.23$$

$$R = \frac{\rho_p L_p}{A_p} + \frac{\rho_n L_n}{A_n} \quad 2.24$$

$$K = \frac{k_p A_p}{L_p} + \frac{k_n A_n}{L_n} \quad 2.25$$

where α, R and K are the total Seebeck coefficient: electrical resistance and thermal conductance of the couple, respectively. Simplifying Eqns 2.21and 2.22, using Eqns.2.23 to 2.25 gives

$$\dot{Q}_1 = \alpha T_1 I - \frac{1}{2}I^2 R + K(T_1 - T_2) \quad 2.26$$

$$\dot{Q}_2 = \alpha T_2 I + \frac{1}{2}I^2 R + K(T_1 - T_2) \quad 2.27$$

The above two Eqns.2.26 and 2.27 are known as the ideal (standard) equations. The first term $\alpha T_1 I$ is the Peltier/Seebeck effect, which is a reversible process. A higher Peltier/Seebeck effect is needed in order to have a higher cooling or power generation. The second term $\frac{1}{2} I^2 R$ is known as the Joule heating, which is an irreversible process. Finally, the third term $K(T_1 - T_2)$ is the thermal conductance, which is also an irreversible process. The heat flow direction is significant in order to know the type of thermoelectric couple, either a thermoelectric cooler or thermoelectric generator. If the direction of heat flow is same as the direction that shows in Figure 2-2 then it represents the thermoelectric generator. By reversing the heat flow direction, the thermoelectric cooler can be represented.

2.2.3 Thermoelectric generator (TEG)

A thermoelectric generator is a power generating device that directly converts thermal energy into electrical energy [13]. When the connected junctions of two dissimilar materials (n-type and p-type) have a temperature difference, an electrical current is generated as shown in Figure 2-3. For a thermoelectric generator, subscript 1 is used for the hot side in equation 2.26 and 2.27 and subscript 2 is used for the cold side.

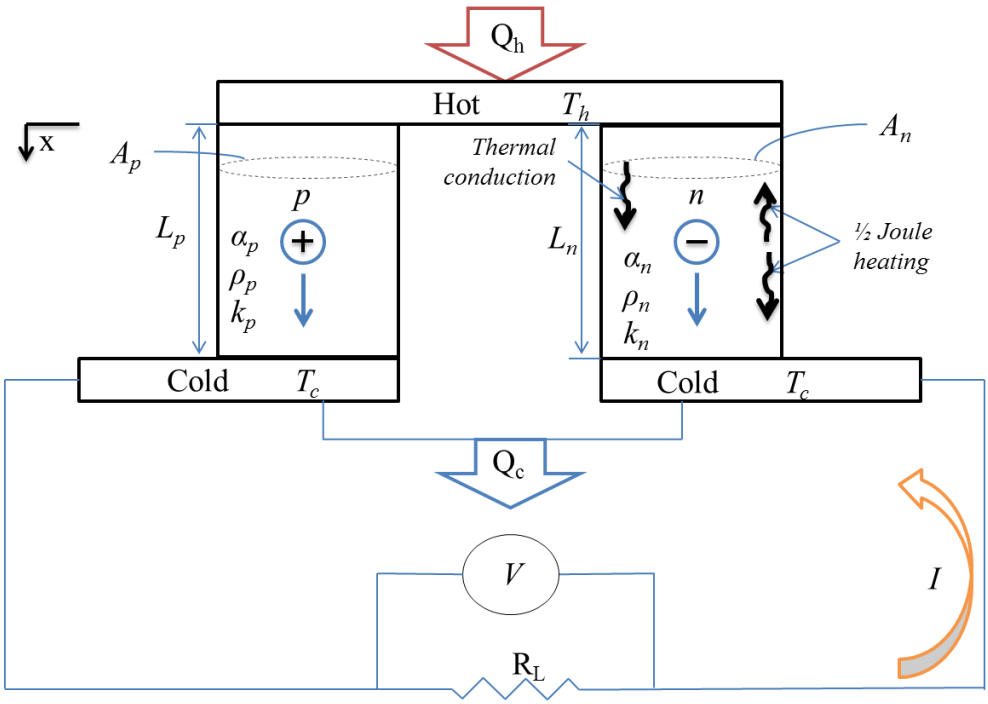

Figure 2-3 An electrical circuit for a unit couple of a thermoelectric generator

$$\dot{Q}_h = \alpha T_h I - \frac{1}{2} I^2 R + K(T_h - T_c) \quad 2.28$$

$$\dot{Q}_c = \alpha T_c I + \frac{1}{2} I^2 R + K(T_h - T_c) \quad 2.29$$

By applying the first law of thermodynamics, the electric power $\dot{W}$ generated from the thermocouple is

$$\dot{W} = \dot{Q}_h - \dot{Q}_c \quad 2.30$$

or

$$\dot{W} = \alpha I(T_h - T_c) - I^2 R \quad 2.31$$

Also,

$$\dot{W} = I^2 R_L \tag{2.32}$$

where R_L is the load resistance. Moreover, Ohm's Law is defined as

$$V = IR_L = \alpha(T_h - T_c) - IR \tag{2.33}$$

Therefore, current I can be written as

$$I = \frac{\alpha(T_h - T_c)}{R_L + R} \tag{2.34}$$

The thermal efficiency of the thermoelectric generator is defined as the ratio of power output to the heat input

$$\eta_{th} = \frac{\dot{W}}{\dot{Q}_h} \tag{2.35}$$

$$\eta_{th} = \frac{I^2 R_L}{\alpha T_h I - \frac{1}{2} I^2 R + K(T_h - T_c)} \tag{2.36}$$

The output power and thermal efficiency can also be rewritten in terms of R_L/R as follows

$$\dot{W} = \frac{\alpha^2 T_c^2 \left[\left(\frac{T_c}{T_h}\right)^{-1} - 1\right]^2 \left(\frac{R_L}{R}\right)}{R\left(1 + \frac{R_L}{R}\right)^2} \tag{2.37}$$

$$\eta_{th} = \frac{\left(1 - \frac{T_c}{T_h}\right)\left(\frac{R_L}{R}\right)}{\left(1 + \frac{R_L}{R}\right) - \frac{1}{2}\left(1 - \frac{T_c}{T_h}\right) + \frac{\left(1 + \frac{R_L}{R}\right)^2 \frac{T_c}{T_h}}{ZT_c}} \tag{2.38}$$

For maximum conversion efficiency

$$\frac{d\eta_{th}}{d\left(\frac{R_L}{R}\right)} = 0 \quad \xrightarrow{gives} \quad \frac{R_L}{R} = \sqrt{1 + Z\bar{T}} \tag{2.39}$$

where $\bar{T}$ is the average temperature between the hot and cold junction and is equal to

$$\bar{T} = \frac{T_c + T_h}{2} = \frac{1}{2} T_c \left[1 + \left(\frac{T_c}{T_h}\right)^{-1}\right] \tag{2.40}$$

As a result, the maximum conversion efficiency, η_{mc}, is

$$\eta_{mc} = \left(1 - \frac{T_c}{T_h}\right) \frac{\sqrt{1 + Z\bar{T}} - 1}{\sqrt{1 + Z\bar{T}} + \frac{T_c}{T_h}} \tag{2.41}$$

For maximum power efficiency

$$\frac{d\dot{W}}{d\left(\frac{R_L}{R}\right)} = 0 \quad \xrightarrow{gives} \quad \frac{R_L}{R} = 1 \tag{2.42}$$

As a result, the optimum current I_{mp}, maximum power $\dot{W}_{max}$ and maximum power efficiency η_{mp}, are

$$I_{mp} = \frac{\alpha \Delta T}{2R} \tag{2.43}$$

$$\dot{W}_{max} = \frac{\alpha^2 \Delta T^2}{4R} \tag{2.44}$$

$$\eta_{mp} = \frac{\left(1 - \frac{T_c}{T_h}\right)}{2 - \frac{1}{2}\left(1 - \frac{T_c}{T_h}\right) + \frac{4\frac{T_c}{T_h}}{ZT_c}} \quad 2.45$$

It can be seen from the above equations that the maximum parameters I_{mp}, $\dot{W}_{max}$, and η_{mp} are independent of the load resistance R_L. Therefore, these maximum parameters can be used to generate a generalized graph for TEG as a function of load resistance where output power, voltage, electrical current, and thermal efficiency obtained from equations 2.32,2.33,2.34 and 2.36 respectively, are divided by maximum parameters as shown Figure 2-4. It can be seen from the plot that the maximum output power is when the load resistance is equal to the internal resistance of the thermoelectric couple. Moreover, the thermal efficiency curve follows the same trend of the output power but its maximum value does not appear when the load resistance is equal to the internal resistance.

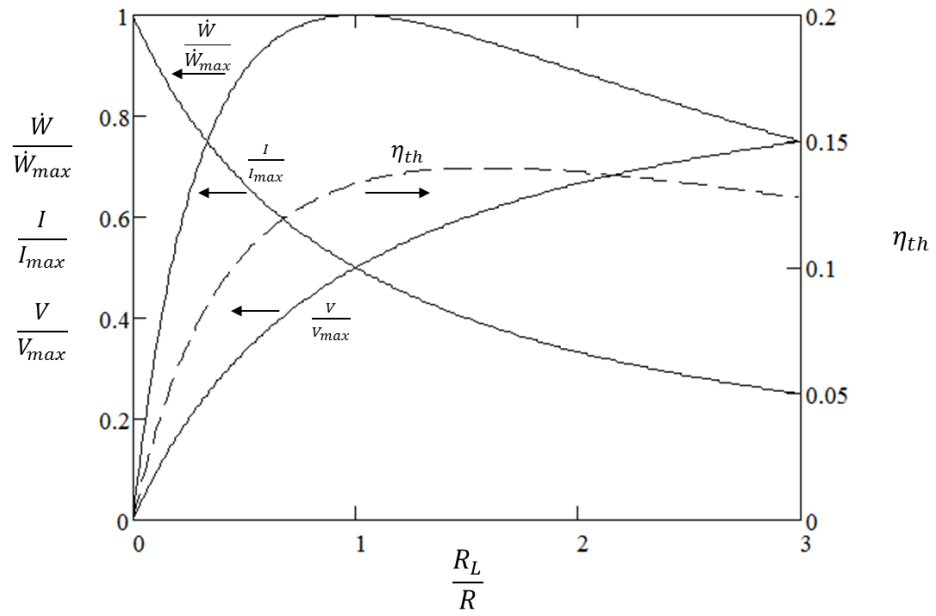

Figure 2-4 Generalized chart of TEG characteristics where ZT=1

This analysis represents the concepts of the thermoelectric generator of one thermocouple where multiple couples are being used in many of the TEG applications. In order to obtain the thermoelectric parameters for multiple couples as shown in Figure 2-5, the unit couple parameters need to be multiplied by the number of couples, n, as follows

$$\left(\dot{W}\right)_{no} = n\dot{W} \quad 2.46$$

$$\left(\dot{Q}_h\right)_{no} = n\dot{Q}_h \quad 2.47$$

$$(R)_{no} = nR \quad 2.48$$

$$(R_L)_{no} = nR_L \quad 2.49$$

$$(V)_{no} = nV \quad 2.50$$

$$(K)_{no} = nK \quad 2.51$$

$$(I)_{no} = I \tag{2.52}$$

$$(\eta_{th})_{no} = \frac{(\dot{W})_{no}}{(\dot{Q}_h)_{no}} = \eta_{th} \tag{2.53}$$

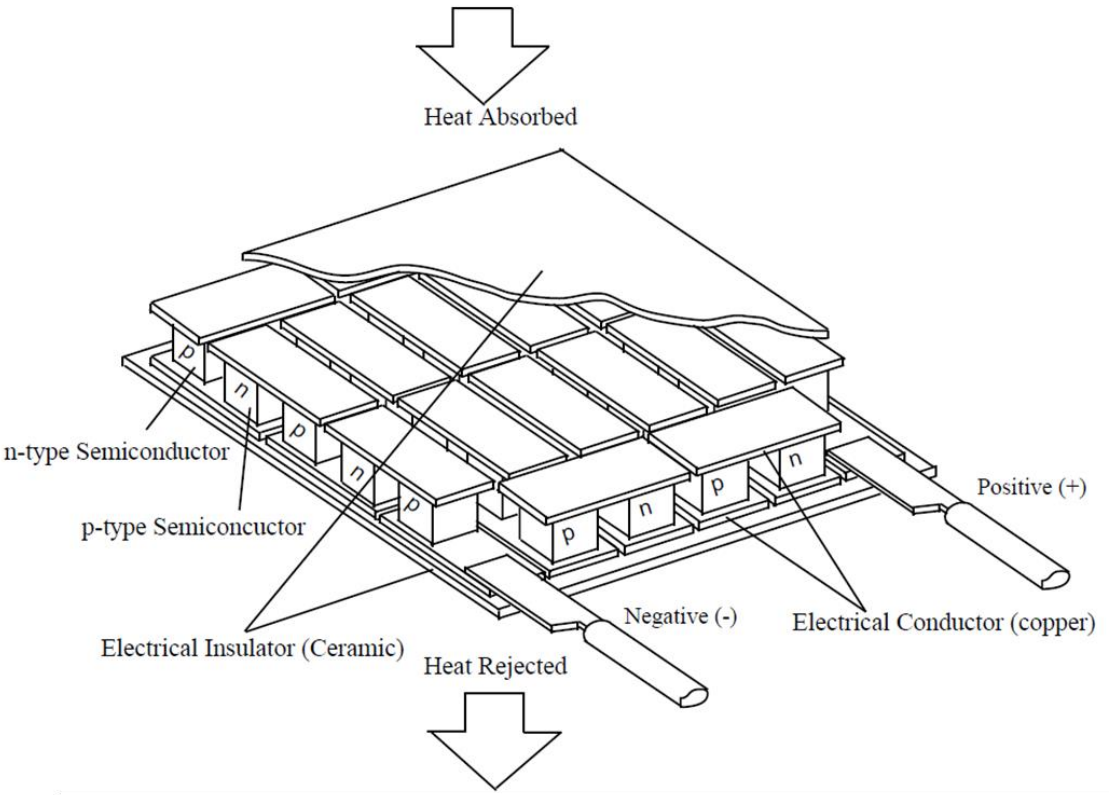

Figure 2-5 A conventional thermoelectric module

2.2.4 Thermoelectric cooler (TEC)

The Seebeck effect is a reversible process. If a current is supplied to a thermoelectric couple, electrons and holes will move through *p* and *n* elements causing heating on one side and cooling on the other as shown in Figure 2-6.

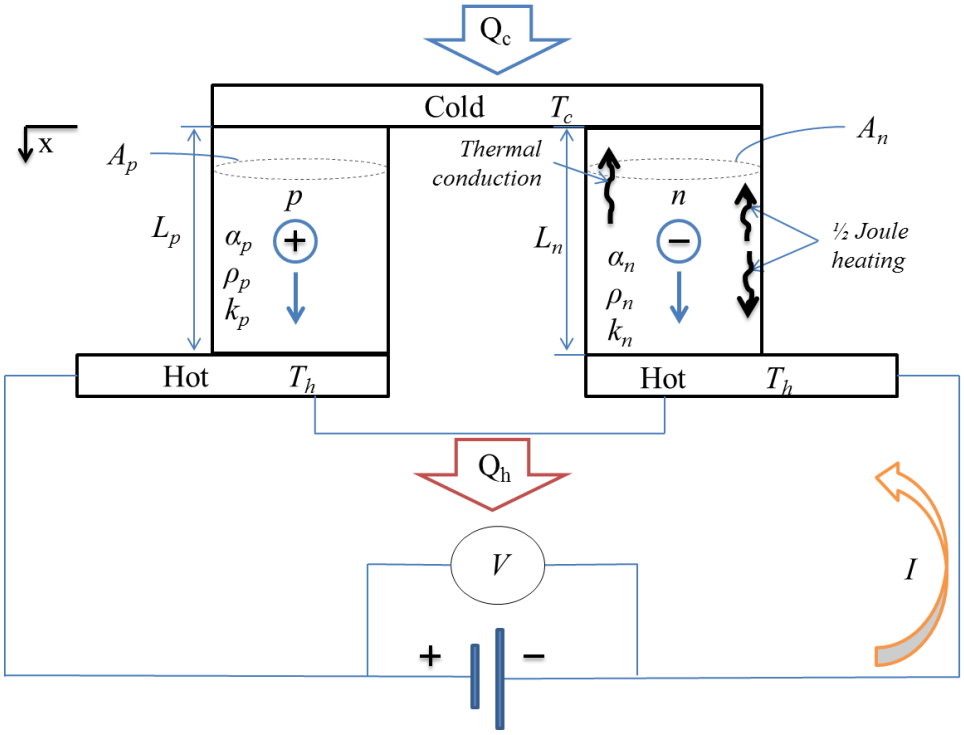

Figure 2-6 A thermoelectric cooler couple

For thermoelectric cooling, subscript 1 is generally used to denote the cold side and subscript 2 is used to denote the hot side which gives [14]

$$\dot{Q}_c = \alpha T_c I - \frac{1}{2} I^2 R + K(T_c - T_h) \qquad 2.54$$

$$\dot{Q}_h = \alpha T_h I + \frac{1}{2} I^2 R + K(T_c - T_h) \qquad 2.55$$

By applying the first law of thermodynamics across the thermocouple, the input power can be defined as

$$\dot{W} = \dot{Q}_h - \dot{Q}_c \qquad 2.56$$

which is also equal to

$$\dot{W} = \alpha I(T_h - T_c) + I^2R \quad 2.57$$

also,

$$\dot{W} = IV \quad 2.58$$

Hence, voltage becomes

$$V = \alpha(T_h - T_c) + IR \quad 2.59$$

The coefficient of performance COP is similar to the thermal efficiency but its value may be greater than 1 and it is defined as the ratio of the cooling power (or heating power) to the input power [14].

$$COP = \frac{\dot{Q}_c}{\dot{W}} \quad 2.60$$

Substituting Equations 2.54 and 2.54 and 2.55 into 2.592.57 gives [15]

$$COP = \frac{\alpha T_c I - \frac{1}{2}I^2R - K\Delta T}{\alpha I \Delta T + I^2R} \quad 2.61$$

where

$$\Delta T = (T_h - T_c) \quad 2.62$$

For maximum cooling power, $\dot{Q}_{c,mp}$, the optimum input current can be found by differentiating Equation 2.542.54 with respect to current and setting it to zero as follows [15]

$$\frac{d\dot{Q}_c}{dI} = \alpha T_c - IR = 0 \xrightarrow{gives} I_{mp} = \frac{\alpha T_c}{R} \quad 2.63$$

The current in Equation 2.63 can also be represented in terms of T_h [15]

$$I_{max} = \frac{\alpha(T_h - \Delta T_{max})}{R} \quad 2.64$$

The maximum temperature difference ΔT_{max} is the maximum possible difference in temperature which always occurs when the cooling power is at zero and the current is maximum. This is obtained by setting $\dot{Q}_c = 0$ in Equation 2.54 substituting both I and T_c by I_{max} and$T_h - \Delta T_{max}$, respectively, and solving forΔT_{max}. The maximum temperature difference is obtained as [15]

$$\Delta T_{max} = \left(T_h + \frac{1}{Z}\right) - \sqrt{\left(T_h + \frac{1}{Z}\right)^2 - T_h^2} \qquad 2.65$$

where the figure of merit Z (unit: K^{-1}) is defined as [15]

$$Z = \frac{\alpha^2}{\rho k} = \frac{\alpha^2}{RK} \qquad 2.66$$

The maximum cooling power $\dot{Q}_{c,max}$ is the maximum thermal load which occurs at $\Delta T = 0$ and $I = I_{max}$. This can be obtained by substituting both I and T_c in Equation 2.54 by I_{max} and $T_h - \Delta T_{max}$, respectively,, and solving for $\dot{Q}_{c,max}$. The maximum cooling power for a thermoelectric module with n thermoelectric couples is [15]

$$\dot{Q}_{c,max} = \frac{n\alpha^2(T_h - \Delta T_{max})}{2R} \qquad 2.67$$

The maximum voltage is the DC voltage which delivers the maximum possible temperature difference ΔT_{max} when $I = I_{max}$. The maximum voltage is obtained from Equation 2.59, which is [15]

$$V_{max} = n\alpha T_h \qquad 2.68$$

The maximum COP can be obtained by differentiating Equation 2.61 with respect to current and setting it to zero as follows [15]

$$\frac{d(COP)}{dI} = 0 \xrightarrow{gives} I_{COP} = \frac{\alpha \Delta T}{R\left[(1+Z\bar{T})^{\frac{1}{2}} - 1\right]} \tag{2.69}$$

$$COP_{max} = \frac{T_c}{T_h - T_c} \frac{(1+Z\bar{T})^{\frac{1}{2}} + \frac{T_h}{T_c}}{(1+Z\bar{T})^{\frac{1}{2}} + 1} \tag{2.70}$$

where

$$Z\bar{T} = ZT_h\left(1 - \frac{\Delta T}{2T_h}\right) \tag{2.71}$$

A dimensionless cooling power ($\dot{Q}_c/\dot{Q}_{c,max}$) and COP vs. dimensionless current (I/I_{max}) can be presented graphically as shown in Figure 2-7 assuming $ZT_c = 1$. The dimensionless cooling power is obtained from the cooling power found in equation (2.542.54), where the current is the only variable, and from the maximum cooling power equation (2.67) at given thermoelectric material properties and hot side temperature. This generalized plot shows that the cooling power is inversely proportional to the coefficient of performance especially at smaller temperature difference. Moreover, increasing the temperature difference across the junction will decrease the cooling power and the performance of the TEC [15].

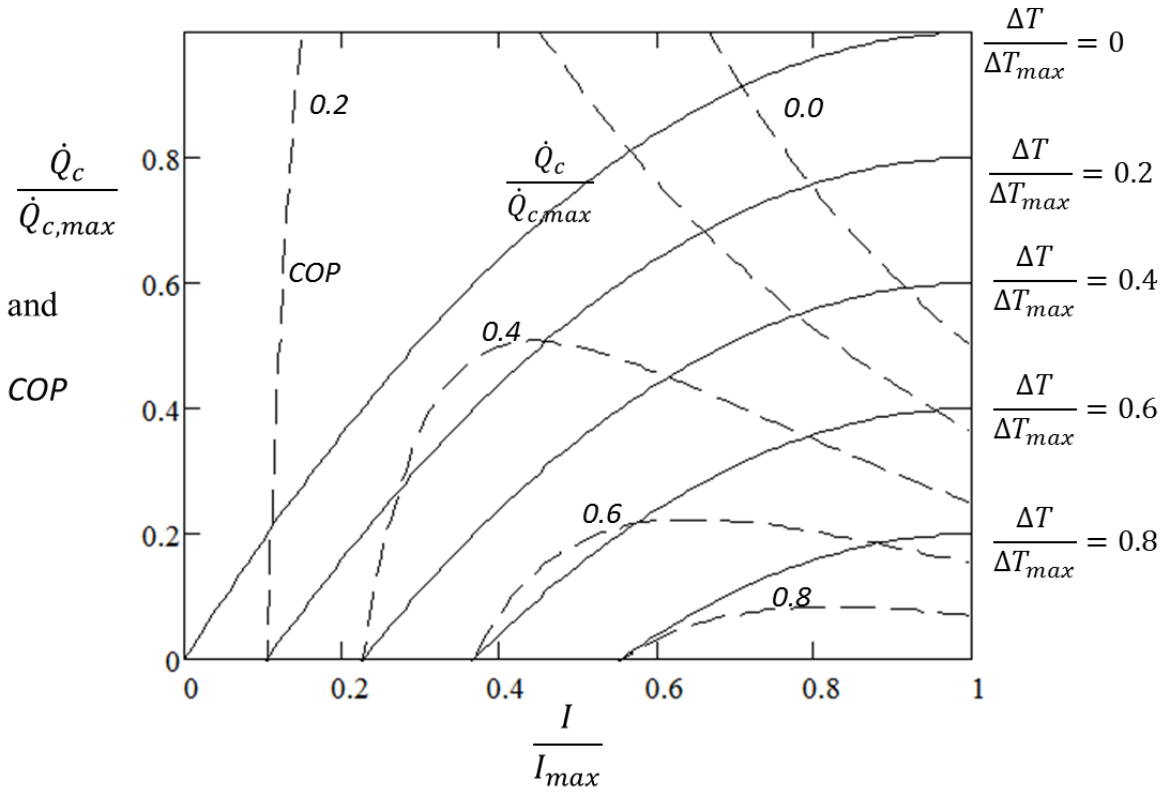

Figure 2-7 Generalized charts for TEC where ZT=1

Similar to the thermoelectric generator, the thermoelectric cooler parameters for multiple couples can be obtained from the unit couple parameters and the number of couples,n as follow [15]

$$\left(\dot{Q}_c\right)_n = n\dot{Q}_c \quad 2.72$$

$$\left(\dot{Q}_h\right)_n = n\dot{Q}_h \quad 2.73$$

$$\left(\dot{W}\right)_n = n\dot{W} \quad 2.74$$

$$(R)_n = nR \quad 2.75$$

$$(V)_n = nV \quad 2.76$$

$$(K)_n = nK \quad 2.77$$

$$(I)_n = I \tag{2.78}$$

$$(COP)_n = \frac{(\dot{Q}_c)_n}{(\dot{W})_n} = COP \tag{2.79}$$

2.2.5 Contact resistances

The thermocouples are usually connected in series by highly conducting metal strips. A number of thermocouples are connected electrically in series and sandwiched between (thermally conducting but electrically insulating) ceramic plates as shown in Figure 2-8. These conductors add electrical and thermal resistances to the system which sometimes increase the discrepancies between the realistic and ideal equation models [16].

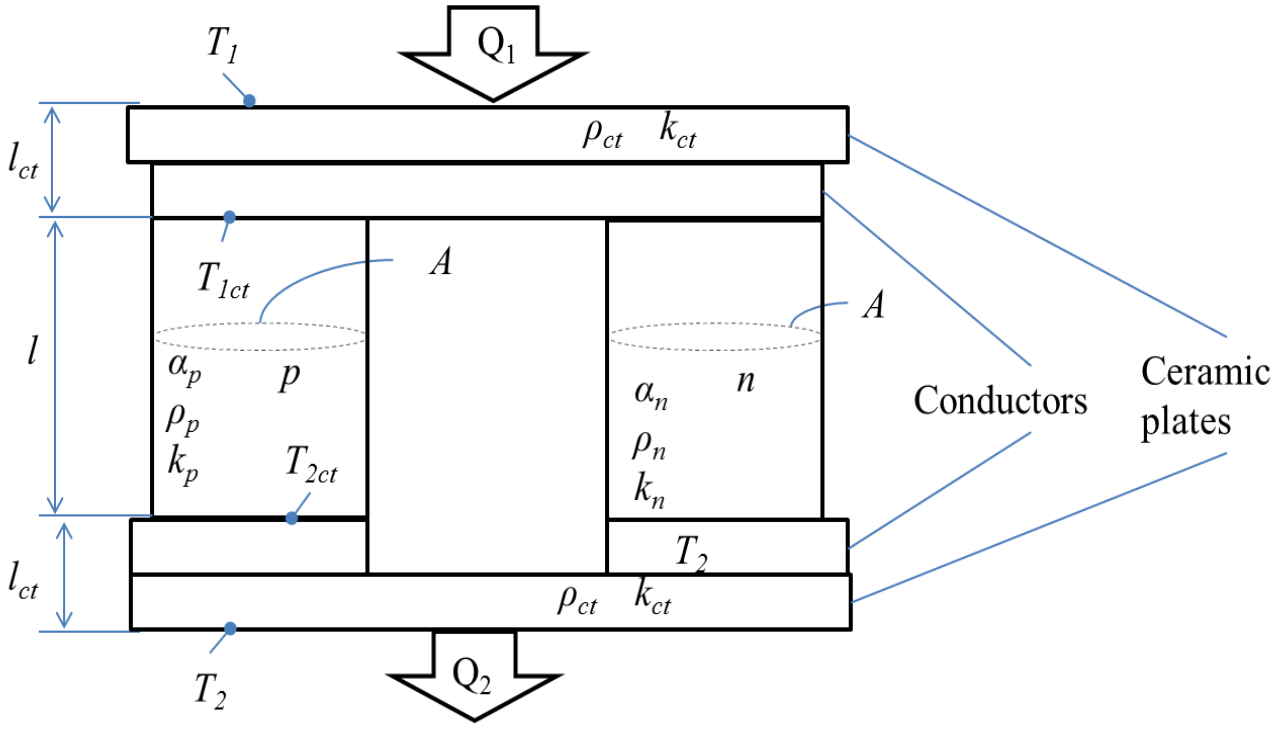

Figure 2-8 A real thermoelectric couple

Consider a single couple thermoelectric cooler where the steady state heat balance can be written as [15]

$$\dot{Q}_1 = \frac{Ak_{ct}}{l_{ct}}(T_1 - T_{1ct}) \tag{2.80}$$

$$\dot{Q}_1 = \alpha I T_{1ct} - \frac{1}{2}I^2R - \frac{Ak}{l}(T_{2ct} - T_{1ct}) \tag{2.81}$$

$$\dot{Q}_2 = \alpha I T_{2ct} + \frac{1}{2}I^2R - \frac{Ak}{l}(T_{2ct} - T_{1ct}) \tag{2.82}$$

$$\dot{Q}_2 = \frac{Ak_{ct}}{l_{ct}}(T_{2ct} - T_2) \tag{2.83}$$

where k_{ct} is the thermal contact conductivity which includes the thermal conductivity of the ceramic plates and thermal contacts and l_{ct} is the thickness of the contact layer. The electrical resistance is composed of the thermocouple and electrical contact resistances as follows [15]

$$R = R_o + R_{ct} = \frac{\rho l}{A} + \frac{\rho_{ct}}{A} = \frac{\rho l}{A}\left(1 + \frac{s}{l}\right) \tag{2.84}$$

where ρ is the electrical resistivity and it is equal to $\rho_n + \rho_p$, ρ_{ct} is the electrical contact resistivity, and s is the ratio between the electrical contact resistivity and electrical resistivity ($s = \rho_{ct}/\rho$). Equations 2.80 to 2.83 are rearranged to have the cooling power per unit area and the coefficient of performance of the TEC module to be [15]

$$\frac{\dot{Q}_1}{nA} = \frac{kT_1}{l}\left[\frac{2Z\bar{T}\xi_{TEC}\left(\frac{T_1}{T_2}+1\right)^{-1}\left(\frac{T_1}{T_2}-1\right)}{\psi\left(1+\frac{s}{l}\right)\left(1-mr\frac{l_c}{l}\right)}\right. \tag{2.85}$$

$$\left. -\frac{Z\bar{T}\left(\frac{T_2}{T_1}+1\right)^{-1}\left(\frac{T_1}{T_2}-1\right)^2}{\psi^2\left(1+\frac{s}{l}\right)\left(1-mr\frac{l_c}{l}\right)^2} - \frac{\left(\frac{T_1}{T_2}-1\right)}{\left(1-mr\frac{l_c}{l}\right)}\right]$$

$$COP$$

$$= \frac{\xi_{TEC}\left(1-mr\frac{l_c}{l}\right)}{\frac{T_2}{T_1}-1}\frac{\left[\psi - \frac{\frac{T_2}{T_1}-1}{2\xi_{TEC}\left(1-mr\frac{l_c}{l}\right)} - \frac{\psi^2\left(\frac{T_2}{T_1}+1\right)\left(1+\frac{s}{l}\right)}{2Z\bar{T}\xi_{TEC}}\right.}{\psi+1} \tag{2.86}$$

where

$$r = k/k_c \tag{2.87}$$

$$m = 2\left(\frac{Z\bar{T}}{\psi\left(1+\frac{s}{l}\right)}-1\right) \tag{2.88}$$

$$\psi = \sqrt{1+Z\bar{T}}-1 \tag{2.89}$$

$$\xi_{TEC} = \frac{T_{1c}}{T_1}$$

$$= \frac{1+\frac{l_c}{l}\frac{Z\bar{T}\left(1+\frac{T_2}{T_1}\right)^{-1}\left(\frac{T_2}{T_1}-1\right)^2}{\psi^2\left(1+\frac{s}{l}\right)\left(1-mr\frac{l_c}{l}\right)^2} + r\frac{l_c}{l}\frac{\left(\frac{T_2}{T_1}-1\right)}{\left(1-mr\frac{l_c}{l}\right)}}{1+2r\frac{l_c}{l}\frac{Z\bar{T}\left(1+\frac{T_2}{T_1}\right)^{-1}\left(\frac{T_2}{T_1}-1\right)}{\psi\left(1+\frac{s}{l}\right)\left(1-mr\frac{l_c}{l}\right)}} \tag{2.90}$$

After studying the above equations, it is found that the effect of the contact resistances increases as the length of the element is decreased. Figure 2-9 shows the cooling power per unit area ($\dot{Q}_1/nA$)

presented in Equation 2.85 and COP (Equation 2.86) as a function of length of the element for four different values of r. The figure implies that the greater the contact resistances the smaller the TEC performances. Moreover, decreasing length of the element implies a greater discrepancy from using the ideal equations (when r and s are equal to zero) especially when length of the element is less than $0.1mm$ [15].

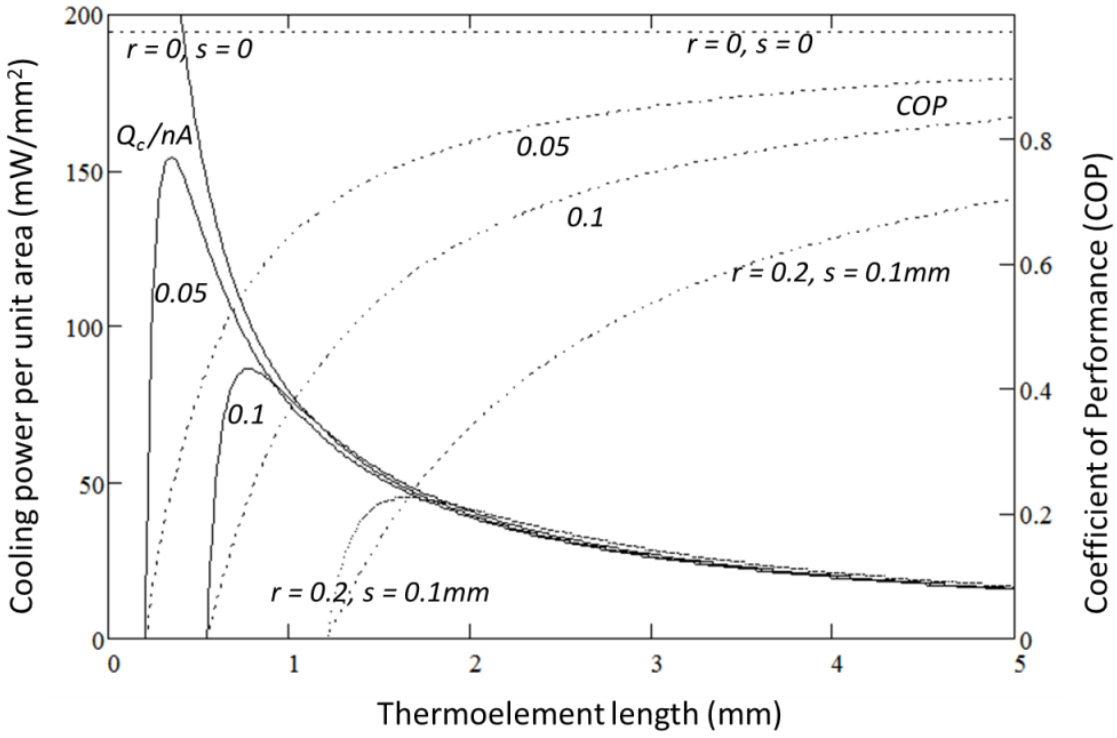

Figure 2-9 Cooling power per unit area and COP as a function of thermo element length

The above figure is for different values of $\boldsymbol{r}$ and when $\boldsymbol{s = 0.1mm}$, $\boldsymbol{\psi = 0.2}$, $\boldsymbol{k = 1.5W/mK}$, $\boldsymbol{l_c = 0.1mm}$, $\boldsymbol{T_1 = 275K}$, $\boldsymbol{T_2 = 300K}$, and $\boldsymbol{Z = 3 \times 10^{-3}\ K^{-1}}$ [15].

2.3 Thermoelectric System

Typical thermoelectric system is usually attached to heat sinks or heat exchanger devices in order to improve the heat absorption and/or rejection. Once these heat sinks are attached, new equations will be considered along with the ideal equations discussed earlier.

2.3.1 Basic equations

Under steady-state heat transfer, consider the thermoelectric cooler system shown in Figure 2-10. Each heat sink faces a fluid flow at temperature T_∞. Subscript 1 and 2 denote the entities of fluid 1 and 2, respectively. Consider that an electric current is directed in a way that the cooling power $\dot{Q}_1$ enters heat sink 1. We assume that the electrical and thermal contact resistances in the TEC are negligible, the material properties are independent of temperature, the TEC is perfectly insulated, and the p-type and n-type element dimensions are identical. [17]

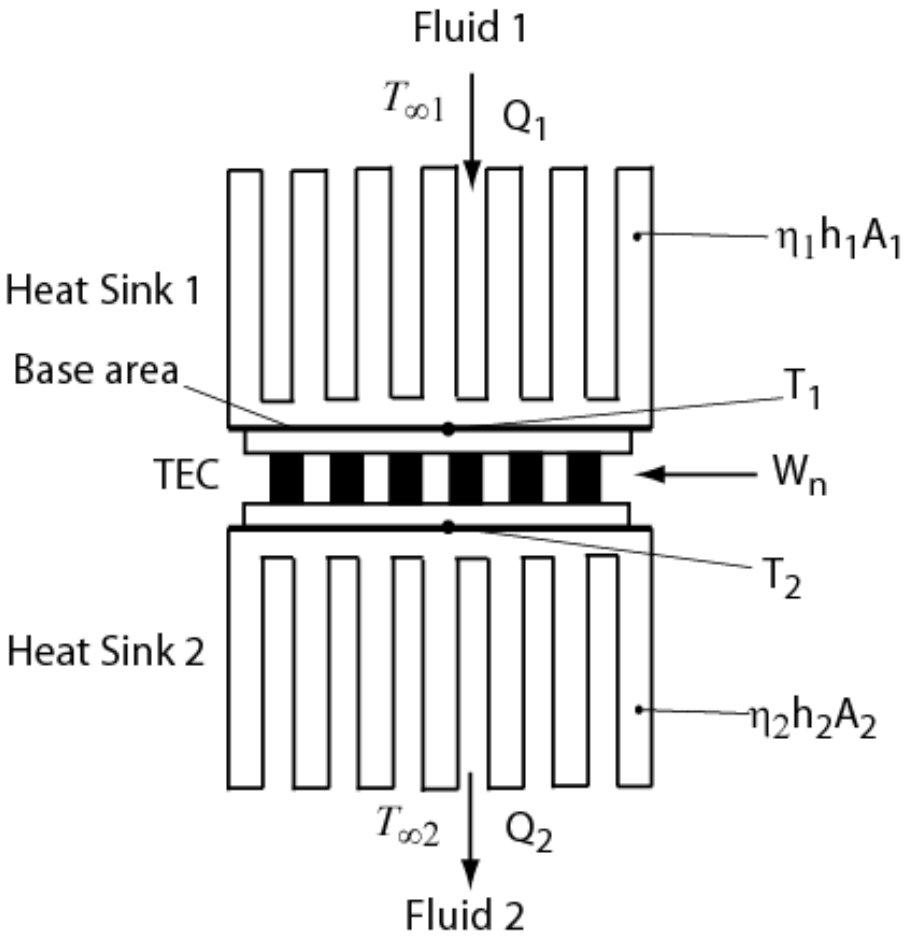

Figure 2-10 Thermoelectric cooler module attached to two heat sinks

The basic equations for the TEC with two heat sinks are given by

$$\dot{Q}_1 = \eta_1 h_1 A_1 (T_{\infty 1} - T_1) \tag{2.91}$$

$$\dot{Q}_1 = n\left[\alpha I T_1 - \frac{1}{2} I^2 R + \frac{A_e k}{L_e}(T_1 - T_2)\right] \tag{2.92}$$

$$\dot{Q}_2 = n\left[\alpha I T_2 + \frac{1}{2} I^2 R + \frac{A_e k}{L_e}(T_1 - T_2)\right] \tag{2.93}$$

$$\dot{Q}_2 = \eta_2 h_2 A_2 (T_2 - T_{\infty 2}) \tag{2.94}$$

It is noted that the thermal resistances of the heat sinks can be expressed by the reciprocal of the convection conductance (i.e., $\eta_1 h_1 A_1$, where η_1 is the fin efficiency, h_1 is the convection coefficient, and A_1 is the total surface area of the cold heat sink). Also, A_e is the element cross-sectional area, L_e is the element length, and T_1 and T_2 are the heat sinks' 1 and 2 base temperatures respectively which are equal to the thermoelectric module junctions temperatures. [18]

2.4 Heat Sink Design and Optimization

The purpose of attaching a heat sink to the thermoelectric module is to maximize the heat transfer rate from the fins. Therefore, at given dimensions (width, W_f, length, L_f, and profile length, b_f) shown in Figure 2-11, the objective of this section is to optimize the fin thickness, t_f, and fin spacing, z_f of a heat sink in order to minimize the thermal resistance. [14]

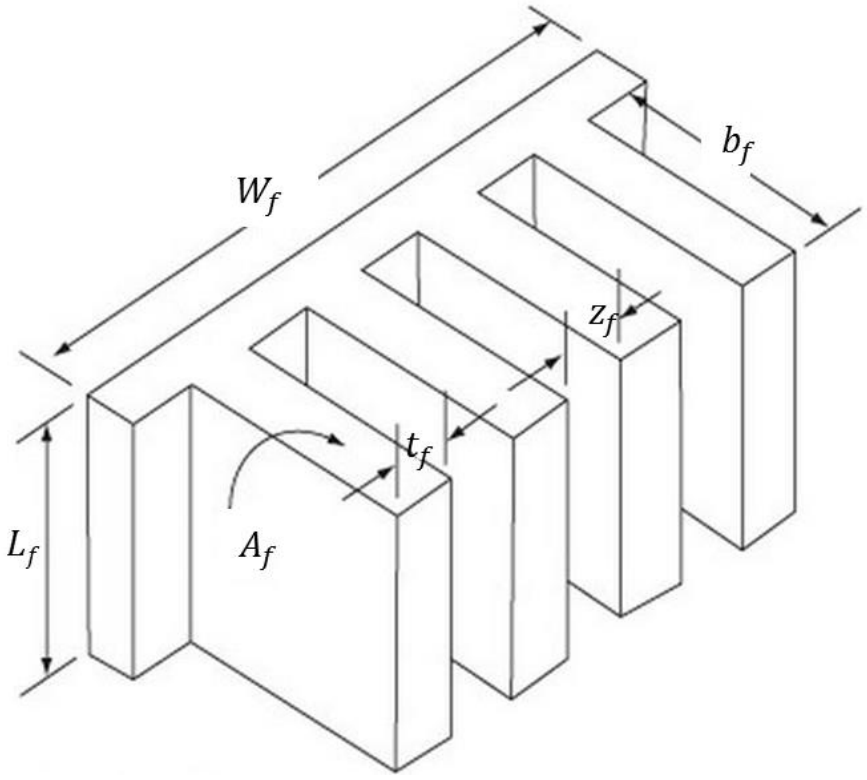

Figure 2-11 Multiple array heat sink

The total fin efficiency is a well-known parameter used to analyze the heat sink thermal resistance and it is defined as follows [15]

$$\eta_f = \frac{\tanh\left[b_f\left(\frac{2h}{k_f t_f}\right)^{1/2}\right]}{b_f\left(\frac{2h}{k_f t_f}\right)^{1/2}} \qquad 2.95$$

where k_f is the thermal conductivity of the fin and h is the heat transfer coefficient of the fluid which can be found from the Nusselt number correlation, Nu, as follow

$$h = \frac{k_{fluid}}{L_f} Nu \qquad 2.96$$

where k_{fluid} is the thermal conductivity of the fluid and L_f is the length of the heat sink that can be replaced by the hydraulic diameter, D_h, for channel flow case. The total heat transfer area of the heat sink is given by

$$A_f = n_f\left[2\left(L_f + t_f\right) + L_f z_{f,opt}\right] \qquad 2.97$$

where n_f is the number of fins. Moreover, it is found that the optimum fin spacing is equal to

$$z_{f,opt} = 3.24 L_f Re_L^{-1/2} Pr^{-1/4} \qquad 2.98$$

where Re_L is the Reynolds number for flow over a plate and Pr is the Prandtl number. After finding the optimum fin spacing for given heat sink parameters, the fin thickness can be optimized to give the maximum heat transfer as follows

$$q_f = \eta_f h A_f (T_\infty - T_b) \qquad 2.99$$

where T_∞ and T_b are the fluid temperatures and the heat sink base temperature respectively [15].

3 LITERATURE REVIEW

There has been a lot of study on TE generators which is mostly based on the concepts of optimization of a heat sink and also on the geometry of TE modules. Some of the studies say that there is enough power generated after optimizing the heat sinks and the others say that there is an increase in power density (power per unit area) with the optimization of the geometry of the TE modules. It all comes down to the procedure used for optimizing their respective set up.

The maximum power output of a TEG is related to three important resistances, the internal TE resistance (thermal and electrical) and the external resistance like the heat sink thermal resistance and the external electrical load resistance. Heat sinks can be optimized with respect to all the resistances if one of them is given. This leads to a simultaneous optimization of the TEG with respect to the external resistances [19]. [19] Explains all the equations related to the optimization of the TEG but does not consider the electrical contact resistance.

[20]This paper proves the effect of thermal (ceramic plate) and electrical contact resistances as mentioned in 2.2.5. It says that the effect of contact resistance is high at low leg lengths. Likewise, at high power density the efficiency of the module goes down. The power produced is almost equal to the ideal case if there is no contact resistances.

In exhaust waste heat recovery systems, there is a lot of insight in the literature which is one of the most important topics in the research fields of TEs. Most of the big automobile manufacturing industries like the General Motors, Nissan Motors, and Porsche etc. are into this [21] [22] [23] [24] [25] [26] [27].

Lee [28] explained the detailed steps in optimizing a heatsink and a thermoelectric module. This method has been verified and can be used for standard ideal equations. Out of many optimization techniques available in literature, the Non-Dimensional technique used in this book is highly effective and its implementation into the ideal thermoelectric modules can also be done without any doubt.

The basic idea of simulation can be obtained from [29]. The procedure to vary load resistance and the concept of varying the resistivity of the load resistance geometry is taken from [30] . This can be an alternate way to vary the load resistance.

The objective of this study is to analyze the effect of thermal and electrical contact resistances of a TEG and to study its importance at low leg lengths and to validate the same using ANSYS.

4 MODELING A THERMOELECTRIC GENERATOR

The modeling of a thermoelectric generator can be divided into the following steps. Each of these steps is discussed in the following section with a description of each.

- 3D CAD model of the TEG
- Specify materials for the model
- Meshing of the model
- Providing inputs
- Simulation

4.1 CAD Modeling

4.1.1 Single module

A 3D model of a module is prepared using the design modeler option in ANSYS. The material of each part in the module is indicated in the following figure.

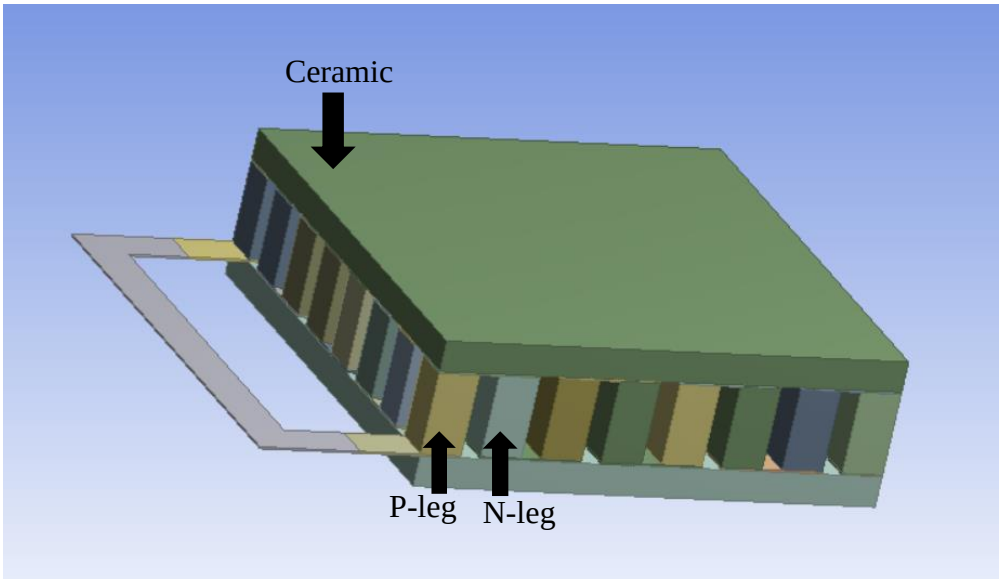

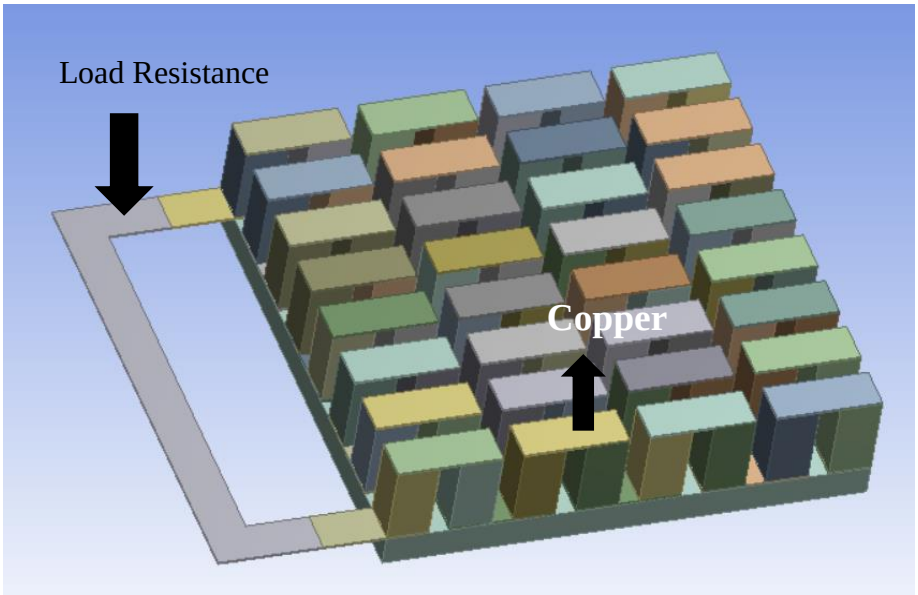

Figure 4-1 3D CAD model of a module

The figures above show the basic design of a thermoelectric generator and the placement of various materials in it like the p type leg, n type leg, electrical copper conductor, load resistance and the ceramic. The module consists of 32 thermoelectric couples and the numerical study is based on varying leg lengths. The effect of all the factors like electric contact resistance, electrical copper resistance and others studied below are based on leg lengths varying from 0.1mm to 1mm.

4.1.2 Modeling with a heat sink

The model was studied using a heatsink. A numerical simulation was done by integrating the CFD-CFX model with the thermoelectric model in ANSYS. The figure below shows a schematic of the thermoelectric generator module integrated with the heatsink.

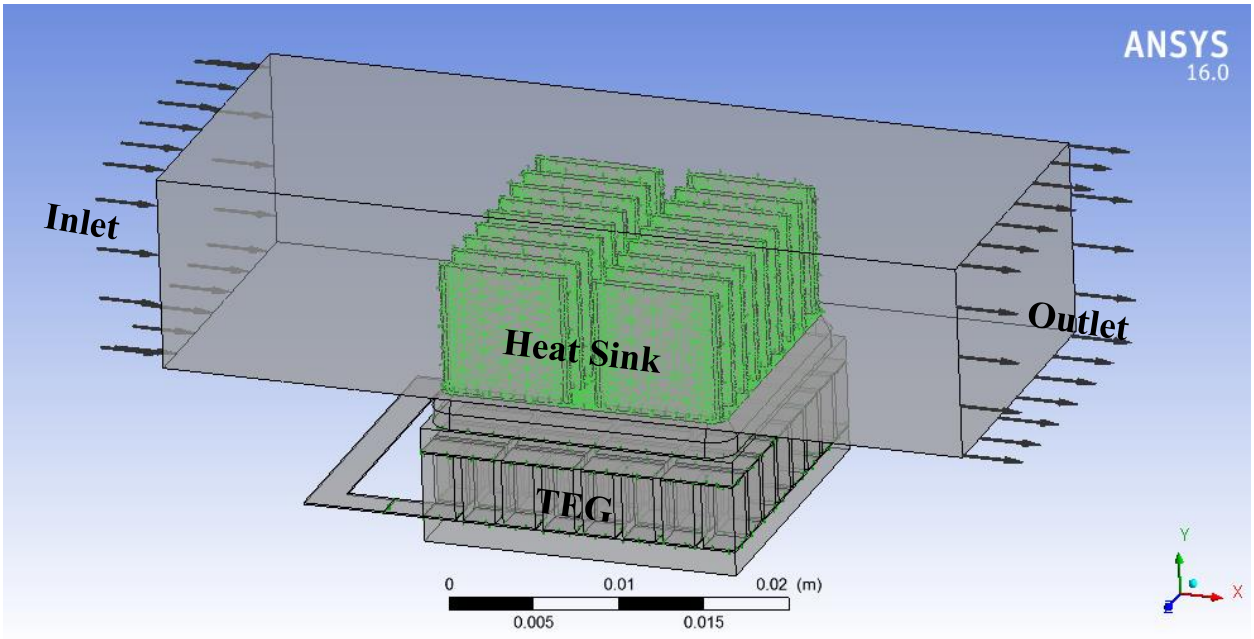

Figure 4-2 Detailed schematic of a TE module coupled with heatsink

4.2 Numerical Simulation of the Module

4.2.1 Assigning materials

Before simulating the given module, material properties needed to be assigned for each geometry in thermal electric model are as shown in Figure 4-3. ANSYS has a standard set of materials in its library. Materials can however, be customized and the properties can be assigned according to the user's requirement.

For the thermoelectric module simulation in ANSYS p-type and n-type material are assigned properties like the isotropic Seebeck coefficient, isotropic thermal conductivity and the isotropic resistivity whereas the ceramic is assigned only the thermal conductivity and the Load Resistance is assigned the electrical conductivity.

For the fluid flow simulation, the CFX module is used in ANSYS. The material used for the heat sink is Aluminum and its thermal conductivity is chosen as 142W/m*K. For fluid flow analysis properties like the molar mass (g/mole), density (kg/m^3), specific heat (J/kg*K), thermal conductivity (W/m*K), electrical conductivity (S/m) are provided.

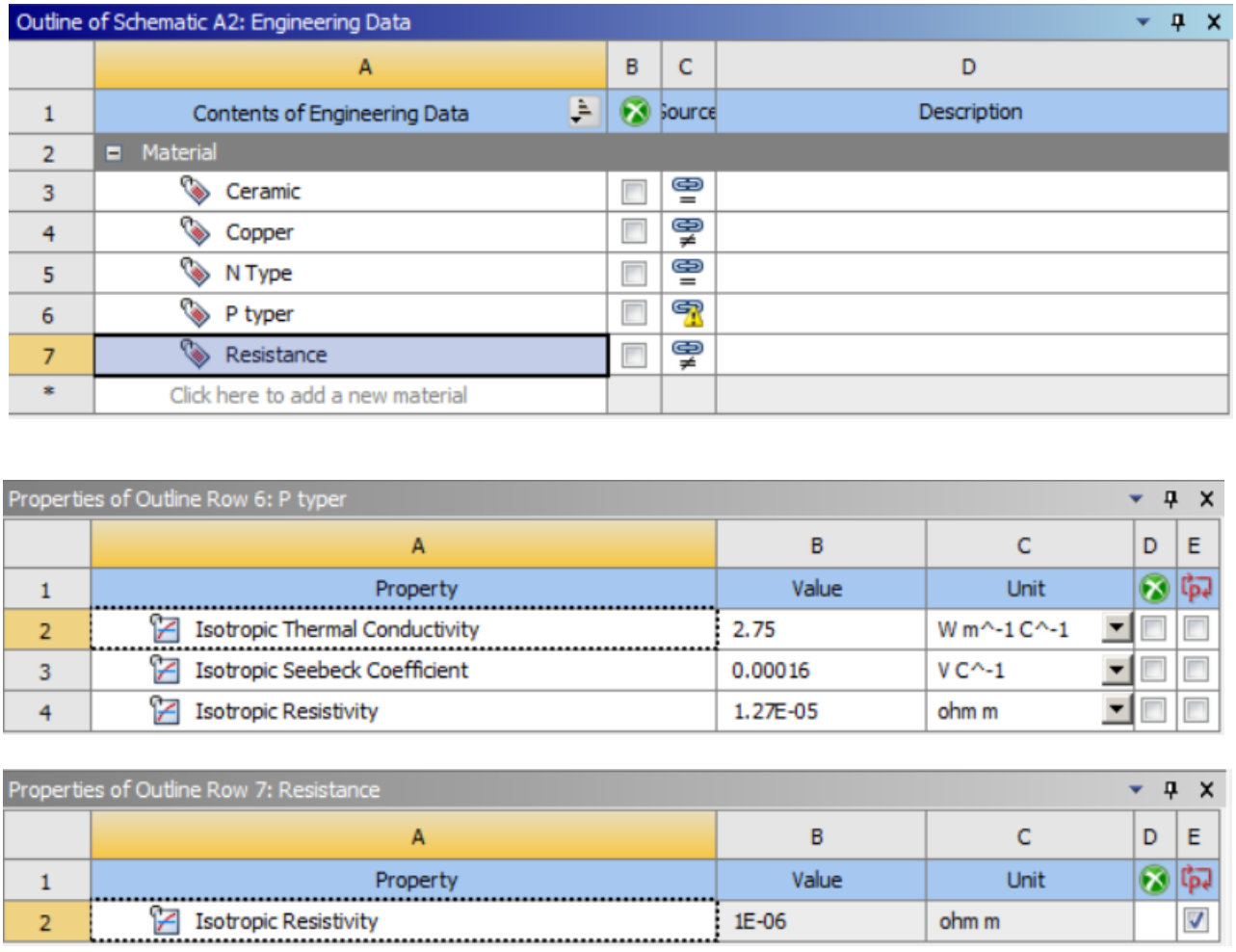

Figure 4-3 Assignment of materials and their properties to a TE module

4.2.2 Meshing

In order to solve the model accurately using ANSYS, meshing plays a very important. Meshing is discretization of the geometry into number of cells and nodes. All the governing equations are

solved in these small discretized nodes. ANSYS Mechanical APDL, thermal-electric module solves using a finite difference method while the CFD-CFX uses a finite volume method. The details of such solutions has been established since the invention of computers and is explained in [31]. In this model, default meshing options have been used and this selection has given dependable results. The figure below shows the meshing that has been used in the software.

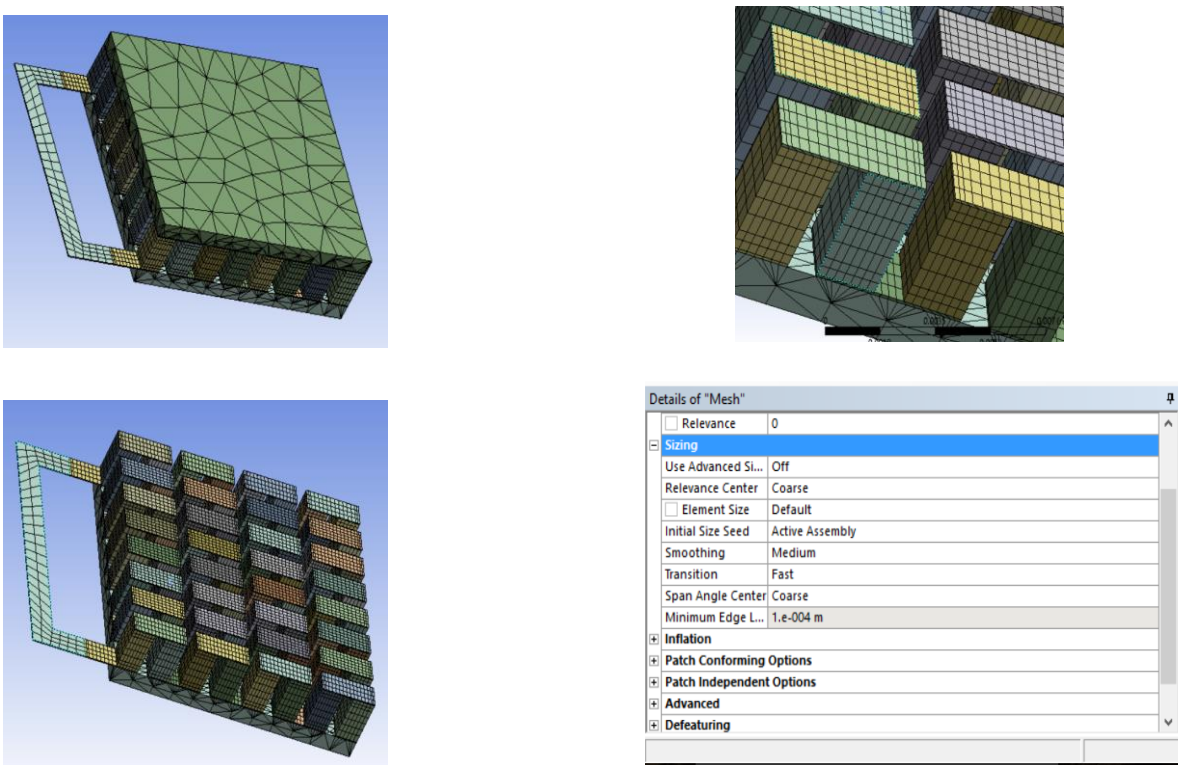

Figure 4-4 Meshing in ANSYS

In the above figure, the top left image shows the module mesh, the mesh chosen is a default mesh, the bottom left image is the same as the top left image but to better understand the internal geometry the ceramic plate is hidden. The top right shows a closer image of the mesh on the thermoelectric legs and the details of the settings of the mesh is shown in the bottom right image.

Mesh size can be changed according to the user requirement. A fine mesh would give better accuracy in the result but would also consume a lot of computing power and time. So there is always an optimum mesh size that a user can define. In this project, the default coarse mesh is chosen since it is sufficient to simulate the problem without consuming a lot of time.

4.2.3 Input data

Once meshing is done and generated for the module, inputs must be given to the module in terms of load resistance, hot side temperature and cold side temperature. The load resistance is given in terms of geometry and the material property of the material used. The regions where these inputs need to be given is shown in the figure below.

When simulating a thermoelectric generator module in ANSYS, it needs three boundary conditions

- Hot temperature
- Cold temperature
- Ground condition or Zero Voltage

ANSYS requires at least one electrical condition as its inputs even though it is not practically needed. This can be specified at any cross section of the electrical circuit as ground condition or the zero voltage. Typically this boundary condition is specified at the cross section of the copper electrical conductor which connects to the load resistance. This is clearly specified in the following fig. as the location ‘C’

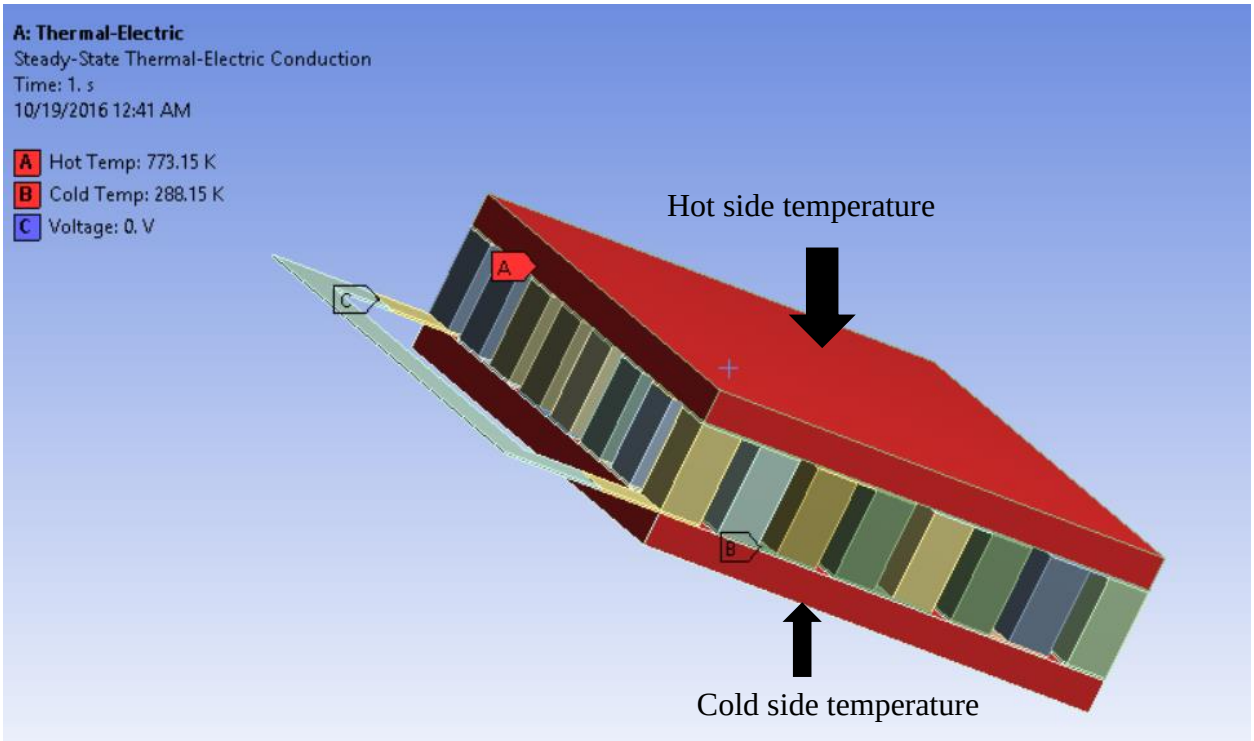

Figure 4-5 ANSYS inputs

4.2.4 Simulation

Simulation of such multiphysics has to be done with a lot of care and understanding. Every node in the mesh has to be simulated for both thermal and electrical governing equations. The thermal conduction, joule heating and the seebeck heat has to be simulated simultaneously. ANSYS has a thermal-electric module in its workbench that includes all the required physics. All the governing equations explained in the previous sections are integrated in this model and this is clearly explained in the ANSYS Help Viewer, Mechanical APDL, Coupling, and Thermoelectrics. [32]

But for coupling the fluid flow and the thermoelectrics, there is no model in ANSYS workbench. This has to be done manually or by the workbench interface. In this project the coupling of such physics is done by the workbench interface and is explained in detail in the results section. Such coupling involves three physics to be solved simultaneously, fluid flow, thermal and the electrical.

CFX model in the workbench of ANSYS is used to solve the fluid flow problem. The governing equations of the CFX and its background is explained in the [33].

This project deals with the optimum in load resistance for every leg length of the thermoelectric element. This calls for a change in the load resistance value which has been controlled by the change in electrical resistivity of the load resistance material there by keeping its geometry constant [34] .

4.3 Analytical Modeling

4.3.1 Analytical modeling without heatsink

An analytical model using MathCad is done in order to compare the results obtained using ANSYS simulations. The equations have been verified and presented in [28]. The equations used are shown below.

$$K_1 \cdot (T_{cj} - T_c) = n \cdot \left[\left[\alpha_e \cdot (I) \cdot T_{cj} + k_e \cdot \frac{A_e}{L_e} \cdot (T_{hj} - T_{cj}) \right] + 0.5 \cdot (I)^2 \cdot \left(\rho_e \cdot \frac{L_e}{A_e} + \rho_{cop} \cdot \frac{L_{cop}}{A_{cop}} + \frac{\rho_c}{A_e} \right) \right]$$

$$K_1 \cdot (T_h - T_{hj}) = n \cdot \left[\left[\alpha_e \cdot I \cdot T_{hj} + k_e \cdot \frac{A_e}{L_e} \cdot (T_{hj} - T_{cj}) \right] - 0.5 \cdot (I)^2 \cdot \left(\rho_e \cdot \frac{L_e}{A_e} + \rho_{cop} \cdot \frac{L_{cop}}{A_{cop}} + \frac{\rho_c}{A_e} \right) \right]$$

$$I = \alpha_e \cdot \frac{(T_{hj} - T_{cj})}{\frac{R_L}{n} + \rho_e \cdot \frac{L_e}{A_e} + \rho_{cop} \cdot \frac{L_{cop}}{A_{cop}} + \frac{\rho_c}{A_e}} \qquad R_{cop} = \rho_{cop} \cdot \frac{L_{cop}}{A_{cop}} \qquad R_{element} = \rho_e \cdot \frac{L_e}{A_e}$$

Figure 4-6 Overview of the equations used for analytical modeling without the heatshink

The thermoelectric equations have been discussed in detail in the previous sections. After understanding the history behind the development of these equations, theory involved in the development and conditions and assumptions, these equations have been used and edited according to the requirement of the current module.

The most important modification in the current model is the electrical copper (ρ_{cop}) and contact resistance (ρ_c) which is added to the electrical circuit and also the thermal conductance of the ceramic materials are used which is added to the thermal circuit (K_1) and is given as follows.

$$K_1 = k_{cer}\frac{A_{cer}}{l_{cer}} \tag{4.1}$$

The values of the ρ_{cop}, ρ_c, k_{cer}, A_{cer} and l_{cer} are specified in the *Table 1*.

4.3.2 Analytical model with heatsink

When a heatsink is involved the enthalpy flow and the convection conductance of the heatsink has to be considered. This can be seen by the addition of two more equations.

$$K_1\cdot(T_{cj}-T_c) = n\cdot\left[\left[\alpha_e\cdot\left[\alpha_e\cdot\frac{(T_{hj}-T_{cj})}{\frac{R_L}{n}+\rho_e\cdot\frac{L_e}{A_e}+\rho_{cop}\cdot\frac{L_{cop}}{A_{cop}}}\right]\cdot T_{cj}+k_e\cdot\frac{A_e}{L_e}\cdot(T_{hj}-T_{cj})\right]+0.5\cdot\left[\alpha_e\cdot\frac{(T_{hj}-T_{cj})}{\frac{R_L}{n}+\rho_e\cdot\frac{L_e}{A_e}+\rho_{cop}\cdot\frac{L_{cop}}{A_{cop}}}\right]^2\cdot\left(\rho_e\cdot\frac{L_e}{A_e}+\rho_{cop}\cdot\frac{L_{cop}}{A_{cop}}\right)\right]$$

$$K_1\cdot(T_h-T_{hj}) = n\cdot\left[\left[\alpha_e\cdot\left[\alpha_e\cdot\frac{(T_{hj}-T_{cj})}{\frac{R_L}{n}+\rho_e\cdot\frac{L_e}{A_e}+\rho_{cop}\cdot\frac{L_{cop}}{A_{cop}}}\right]\cdot T_{hj}+k_e\cdot\frac{A_e}{L_e}\cdot(T_{hj}-T_{cj})\right]-0.5\cdot\left[\alpha_e\cdot\frac{(T_{hj}-T_{cj})}{\frac{R_L}{n}+\rho_e\cdot\frac{L_e}{A_e}+\rho_{cop}\cdot\frac{L_{cop}}{A_{cop}}}\right]^2\cdot\left(\rho_e\cdot\frac{L_e}{A_e}+\rho_{cop}\cdot\frac{L_{cop}}{A_{cop}}\right)\right]$$

$$K_{conv}\cdot\left(\frac{T_{hin}+T_{hout}}{2}-T_h\right) = K_1\cdot(T_h-T_{hj})$$

$$m_{dot}\cdot c_p\cdot(T_{hin}-T_{hout}) = K_{conv}\cdot\left(\frac{T_{hin}+T_{hout}}{2}-T_h\right)$$

Figure 4-7 Analytical modeling with heatsink

In the above figure the subscripts *h* and *c* denote the hot and cold side quantities respectively. As we can see that the convection conductance of the heatsink is considered and is given by

$$K_{conv} = \eta A_s h_{conv} \tag{4.2}$$

Where h_{conv} is the heat transfer coefficient, η is the efficiency and A_s is the total surface area of the heatsink. It has to be noted that the equations for heatsink is added only on the hot side of the TEG whereas the cold side of the TEG is kept at constant temperature (T_c). The heatsink is enclosed in a rectangular air duct which has an inlet temperature (T_{in}), inlet mass flow rate (m_{dot}) and an outlet temperature (T_{out}). The fluid considered to be flowing is air, and its properties vary with respect to the operating temperature which are obtained from [14] .

5 RESULTS AND DISCUSSIONS

All information in this chapter is with respect to the methodologies explained in Ref. [35], [36], [15], and [37]. In this chapter, validation of existing thermoelectric module is done to prove the authenticity of the ideal equations. A comparison is done between the analytical modeling and ANSYS simulation of the modules under various conditions. ANSYS simulation is first done to observe the performance of a thermoelectric generator module under various conditions. The results are then validated using MathCad equations to verify the authenticity of the simulation. Also, the effect of electrical contact resistances and electrical copper resistances are studied. A thermoelectric generator module is studied under the effect of these resistances and also under the effect of a heatsink. This results are discussed in the sections below. All the materials used in this study and their properties and dimensions are mentioned in the table below.

5.1 Input Parameters Needed to Simulate and Model the TEG

Table 1 Input parameters needed to simulate the TEG

Geometry	Value	Units
P type		
Thermal Cross Section Area	2mm*2mm	mm^2
Length	0.1mm-1.5mm	mm
Seebeck Coefficient (α_p)	160	μV/K
Thermal Conductivity (k_p)	2.75	W/m*K
Electrical Resistivity (ρ_p)	$1.27*10^{-3}$	Ω*cm
N type		
Thermal Cross Section Area	2mm*2mm	mm^2
Length	0.1mm-1.5mm	mm
Seebeck Coefficient (α_p)	-160	μV/K
Thermal Conductivity (k_p)	3.7	W/m*K
Electrical Resistivity (ρ_p)	$0.45*10^{-3}$	Ω*cm
Copper Conductor		
Electrical Cross Section Area	0.1mm*2mm	mm^2
Electrical Length	4.5mm	mm
Thermal Conductivity (k_{cop})	401	W/m*k
Electrical Resistivity (ρ_{cop})	$1.67*10^{-5}$	Ω*mm

Table 1 - continued

Ceramic Insulation Thermal Cross Section Area (A_{cer}) Length (L_{cer}) Thermal Conductivity (k_{cer})	 19.5mm*19.5mm 1.5mm 27 (Alumina), 180(AlN)	 mm^2 mm W/m*K
Load Resistance Electrical Cross Section Area Electrical Length Electrical Resistivity	0.1mm*2mm 25.5mm Varies according to the problem	mm^2 mm Ω*m
Contact Material Sheet Electrical Resistivity(ρ_c) (solder material)	 $1.68*10^{-6}$	 $\Omega*cm^2$
Heat sink UB19-10B (Commercial Heat Sink- Aluminum) Thermal Conductivity	[38] 142	___ W/m*K
Air Duct Length Width Depth	 50 19.5 12	 mm mm mm

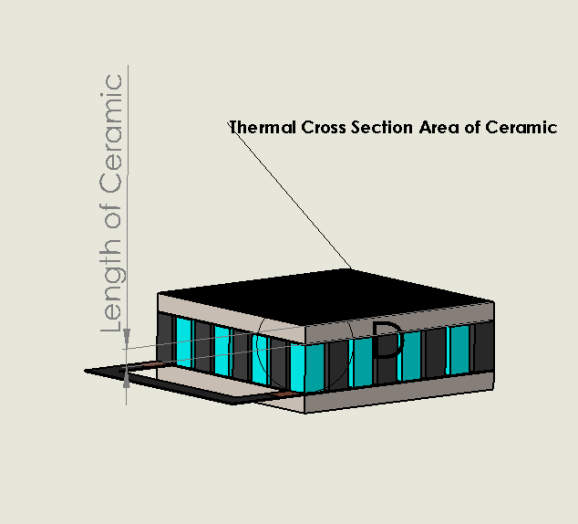

Figure 5-1 Details about the thermal cross section area and the thickness of ceramic

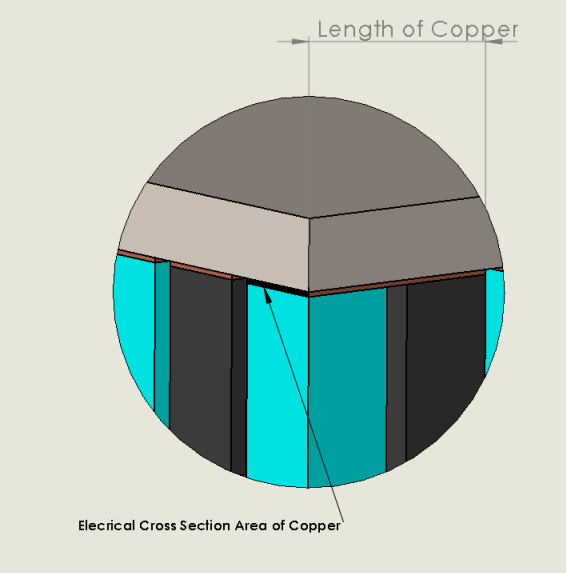

Figure 5-2 Electrical cross section area and length of copper

5.2 Validation of ANSYS and MathCad without Heatsink

The setup of the ANSYS model of a single thermoelectric module has already been discussed in the previous sections. Once the setup is done and simulation is carried out, the results are compared with the theoretical model. In this section, the results from the analytical modeling (Mathcad) are compared with the numerical simulation (ANSYS) which leads to an interesting conclusion. The study discusses the importance of the copper and contact resistance at low leg lengths of the TE materials. Also, the effect of heatsink is studied and observed for the validity of the theoretical model.

5.2.1 Power output at constant leg length

The following graphs show the power generated at constant leg length and at varying load resistance. The ANSYS simulation has been validated using MathCad equations and the results are shown below.

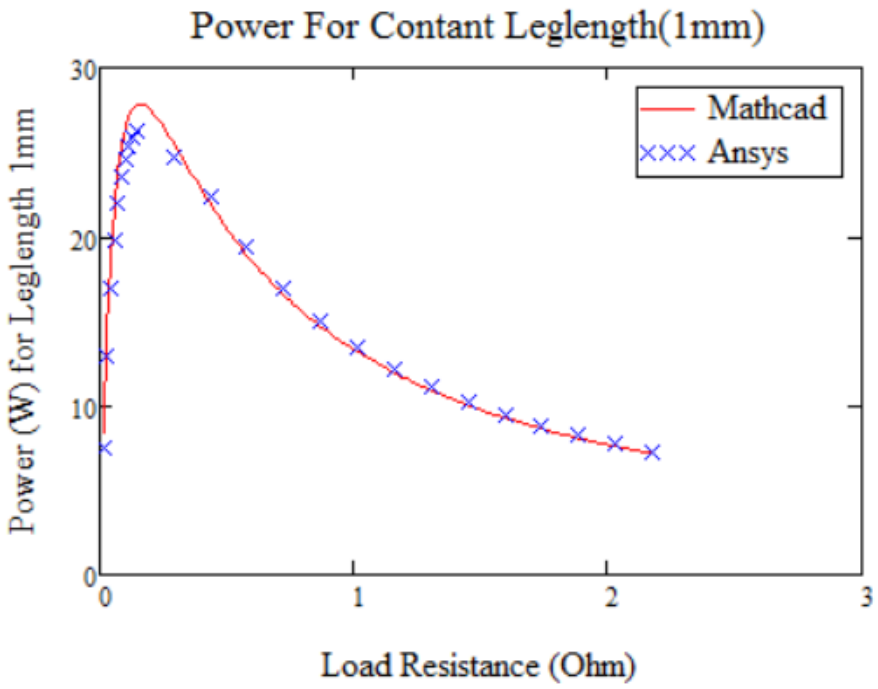

Figure 5-3 Power vs load resistance at constant leg length

The above graph is plotted at hot temperature $\mathbf{T_h = 773K}$, cold temperature $\mathbf{T_c = 288K}$ and the Leg length $\mathbf{L_e = 1mm}$. All the other inputs required are specified in Table 1.

We can see from this graph that there is an optimum value of load resistance where maximum power is reached. It can also be seen that MathCad solution and ANSYS simulated results are in very good agreement with each other. Small discrepancies if any are because of the mesh which has been selected., As discussed earlier, we can see that there is a good agreement in the results despite the size of the mesh selected (course mesh). This may also hold true with all the other graphs that are presented.

5.2.2 Power output at constant load resistacce

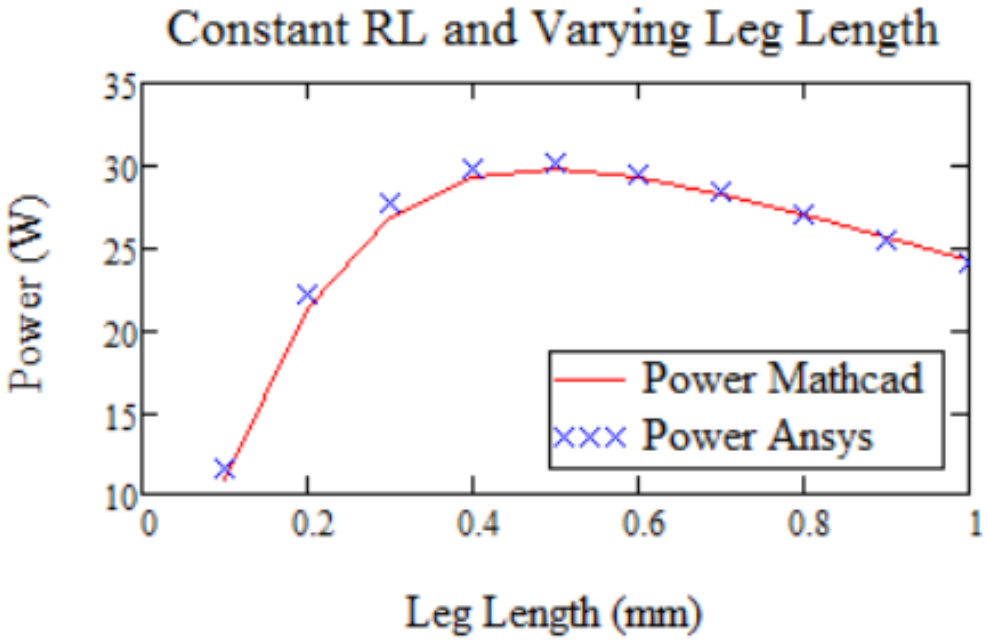

Figure 5-4 Power as a function of leg length at constant load resistance

The above graph is plotted at hot temperature $\mathbf{T_h = 773K}$, cold temperature $\mathbf{T_c = 288K}$ and the Load Resistance $\mathbf{R_L = 0.128\Omega}$ where the resistivity of the load material $\boldsymbol{\rho_{load} = 1*10^{-6}\ \Omega*m}$ and all the other inputs required are specified in Table 1.

In this plot, we can see that the ANSYS simulation is also in good agreement with the analytical data. Also, at a constant load resistance, there is an optimum leg length at which maximum power can be generated out of the module. This is just the opposite graph of Figure 5-3 where the load resistance was constant.

5.2.3 Power output at optimum load resistance

The most commonly used load resistance ratio (ratio of load resistance to internal resistance) value in most of the literature is unity. This value is equal to unity if there are no contact resistances but once the legs are connected to the external contacts like the ceramic plate and the copper conductor the value changes and can be expected to be slightly more than unity. This means that load resistance R_L has an optimum value at different leg lengths. For the simplicity of the problem unity is chosen and the maximum power reached by the module at this value of load resistance ratio at different leg lengths is shown in the plot below.

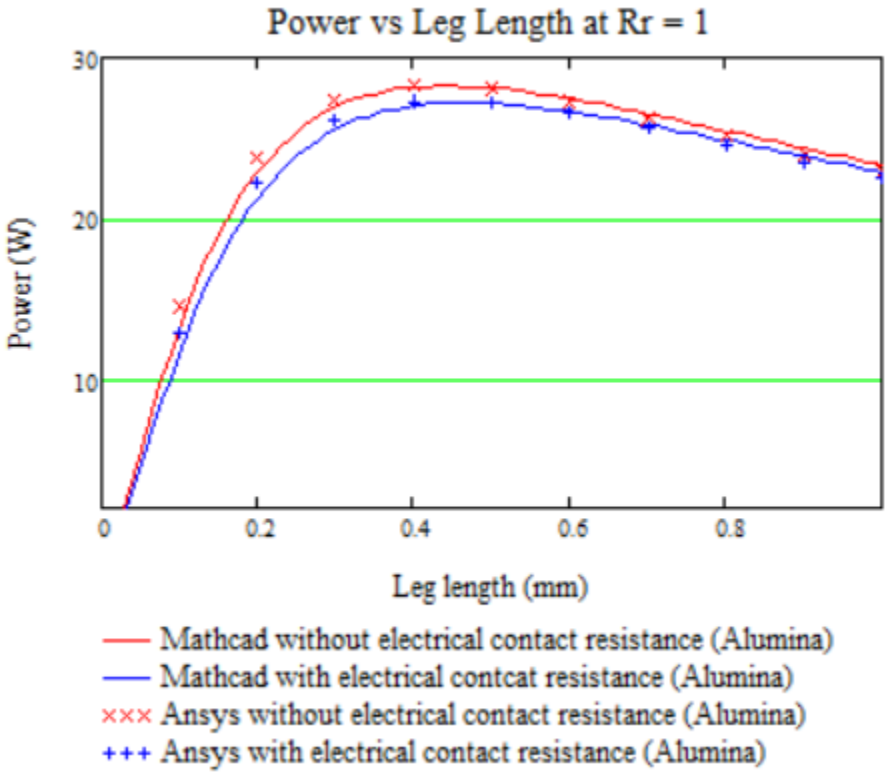

Figure 5-5 Power generated at load resistance ratio =1

The hot temperature is $\mathbf{T_h = 773K}$, cold temperature $\mathbf{T_c = 288K}$ and all the other inputs required are specified in Table 1.

It can be seen from the above figure that the effect of electrical contact resistance is very small. The power output is over predicted in the analytical model which does not include the electrical contact resistance. It can also be seen that the power attains a maximum value with respect to an optimum leg length.

5.2.4 Effect of thermal and electrical contact resistances

The Figure 5-6 shows the performance curve of a thermoelectric generator under various conditions. These conditions include the electrical contact resistances, electrical copper resistances, and the thermal contact resistance (ceramic). The plot shows the change in power generated with change in these conditions.

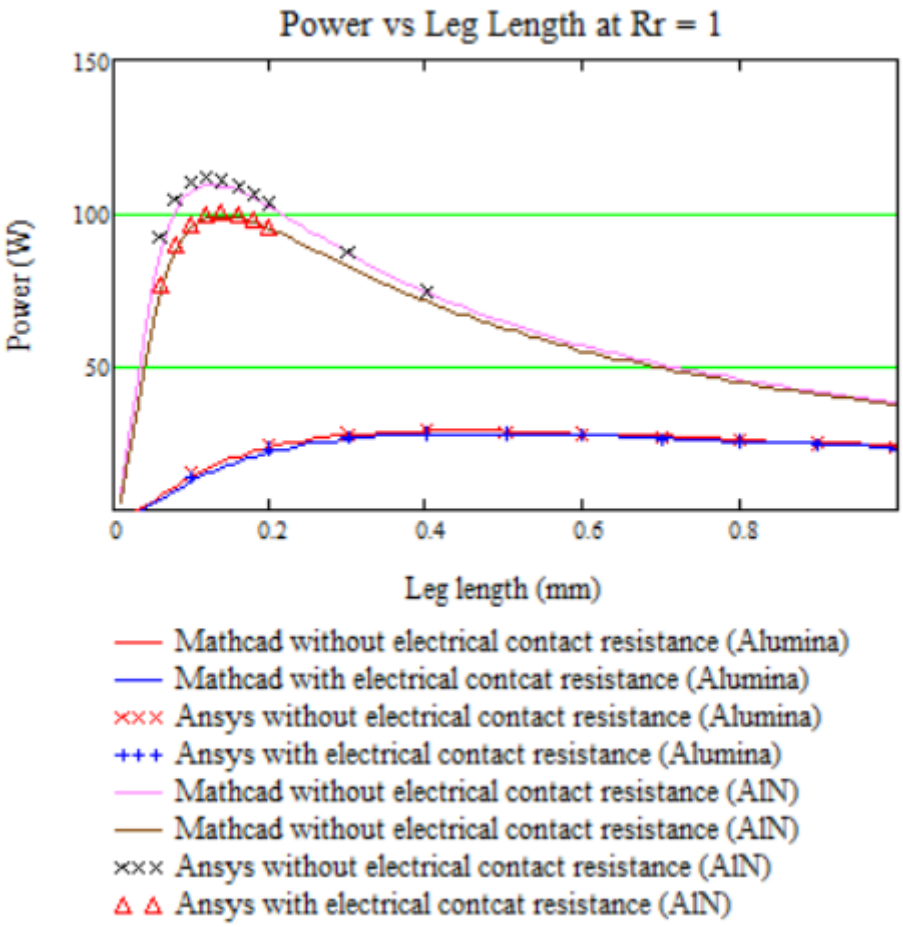

Figure 5-6 Performance curve at different thermal and electrical contact resistance

Inputs for the above figure are taken from Table 1 with hot temperature $\mathbf{T_h = 773K}$, cold temperature $\mathbf{T_c = 288K}$.

The Figure 5-6 shows the importance of the thermal contact material (ceramic) used. The thermal contact material with high thermal conductivity k_c = 180 W/m*K Aluminum Nitride (AlN) shows a dramatic increase in the power output than the material with low thermal conductivity k_c = 27 W/m*K Alumina (Al_2O_3) at low leg lengths.

5.2.5 Importance of electrical copper resistance

As leg length reduces below certain values, the effect of copper resistance increases significantly and at these leg lengths, it becomes important to include the electrical copper resistance. This effect is shown in the figure below.

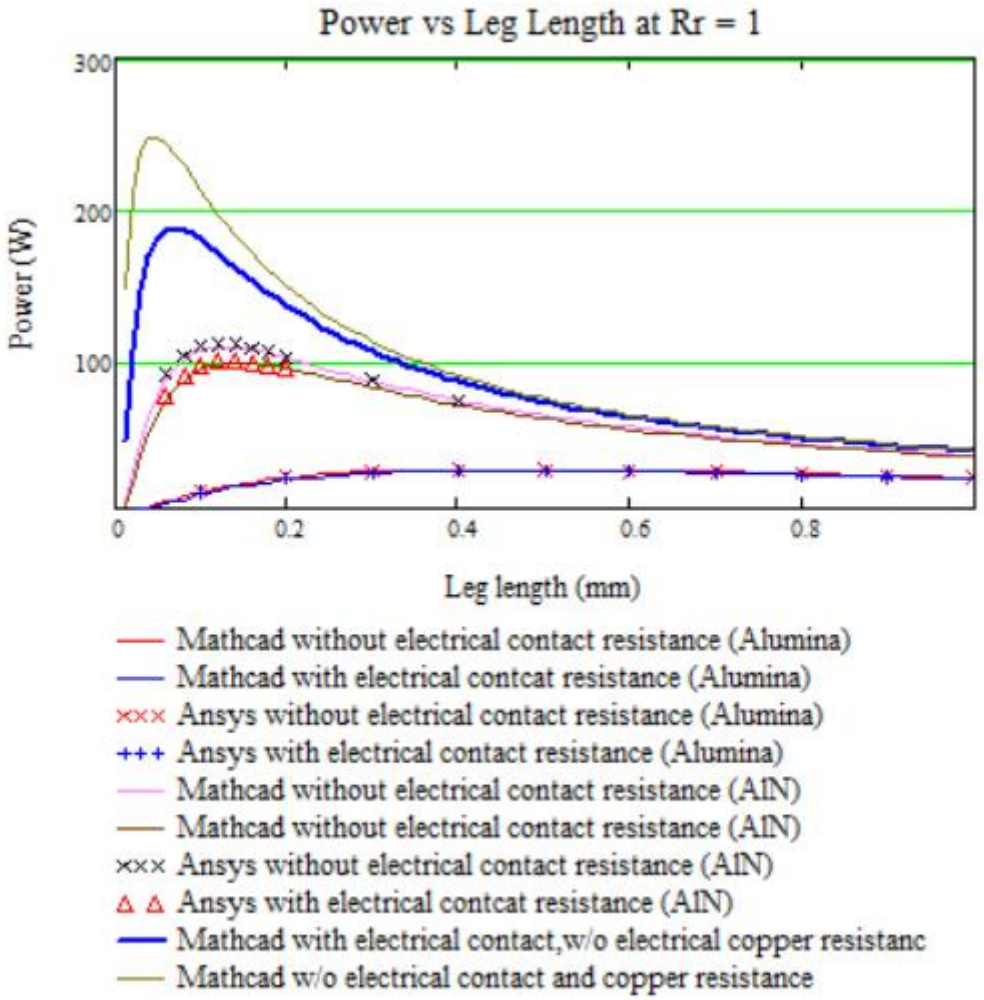

Figure 5-7 Importance of electrical copper resistance

The material properties of all the materials are taken from the Table 1 and the hot temperature $\mathbf{T_h}$ **= 773K**, cold temperature $\mathbf{T_c}$ **= 288K**.

It can be seen form this plot that the electrical copper resistance is very significant at low leg lengths and the power is over predicted when this resistance is not included. The difference is seen to be almost 70W which is huge. Hence, this resistance has to be used while analytically calculating the power generated.

5.2.6 Comparison of ideal power output with real power output

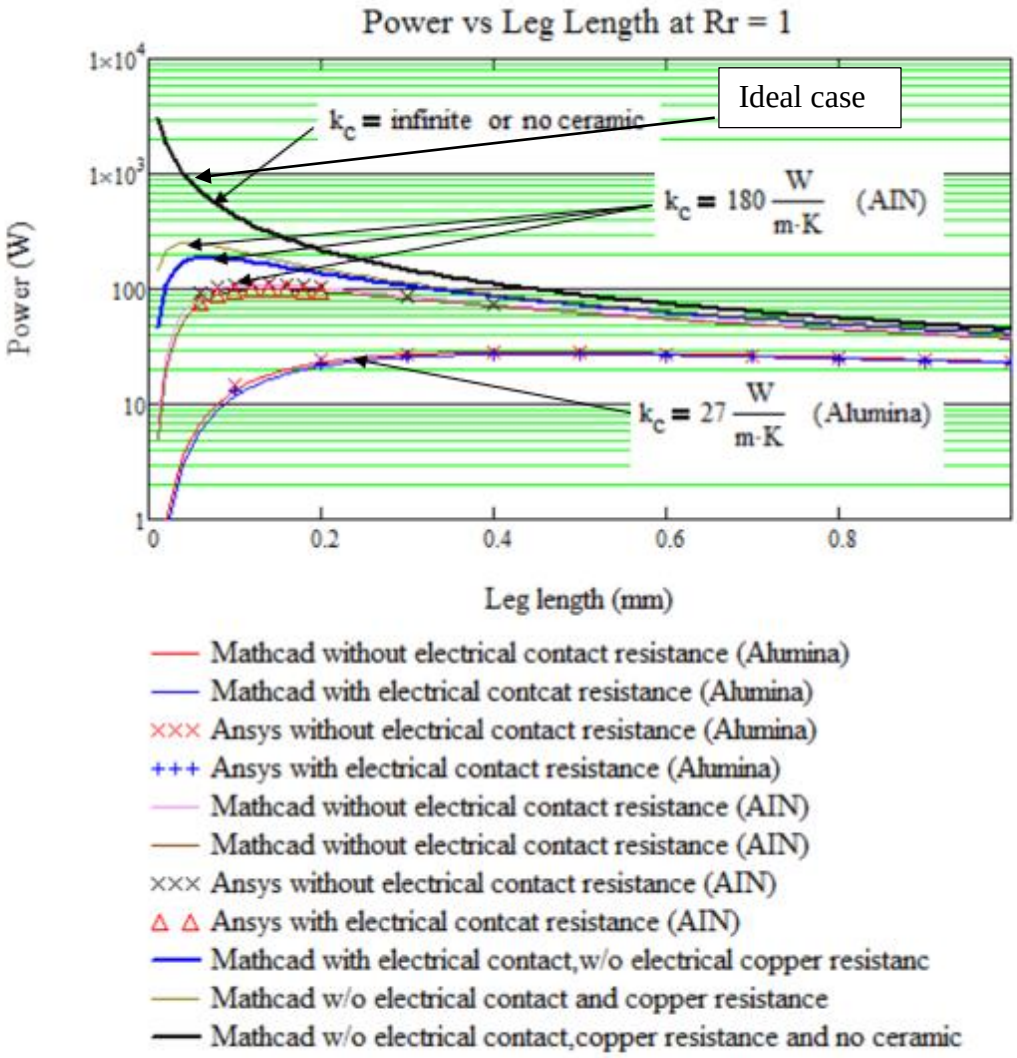

Figure 5-8 Performance curve compared to ideal case

Under ideal cases where ceramic, contact resistance and copper resistances are non-existing i.e. the thermal resistance of ceramic and electrical copper resistance are zero, the MathCad equations

indicate the power generated increases exponentially and doesn't show a drop which is actually not practical. Under practical conditions, where there is always thermal and electrical contact resistance available, there is an optimum value of leg length for which the power generated is maximum. If the leg length is decreased beyond the optimum value there is dramatic drop in power output. This happens at very low leg lengths when such contact resistances are in comparison with the resistance of the legs and hence cannot be ignored.

5.3 Validation of ANSYS and MathCad with Heatsink

5.3.1 ANSYS setup and simulation with heatsink

This section shows the set up and simulation of a TEG with a heatsink as shown in Figure 5-10.

Once the heatsink is set up using CFD-CFX module, boundary conditions are assigned to it in the form of inlet temperature, inlet mass flow rate and pressure outlet as shown in Figure 4-2. The CFX module is initially integrated with the thermal electric module as shown in the following figure;

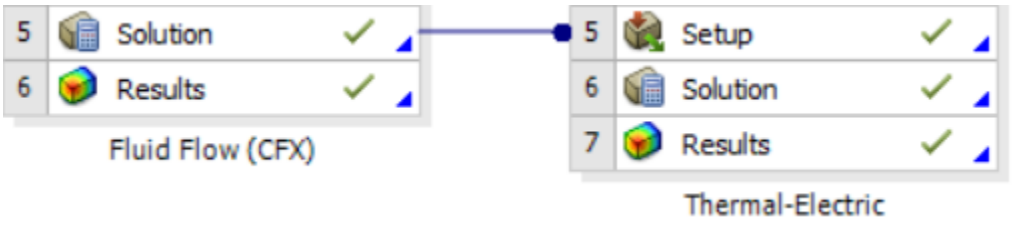

Figure 5-9 Linking the CFX to thermal electric module

5.3.2 Temperature contour across the heatsink

The CFX is solved for the heatsink at the given boundary conditions. The temperature contour is as follows.

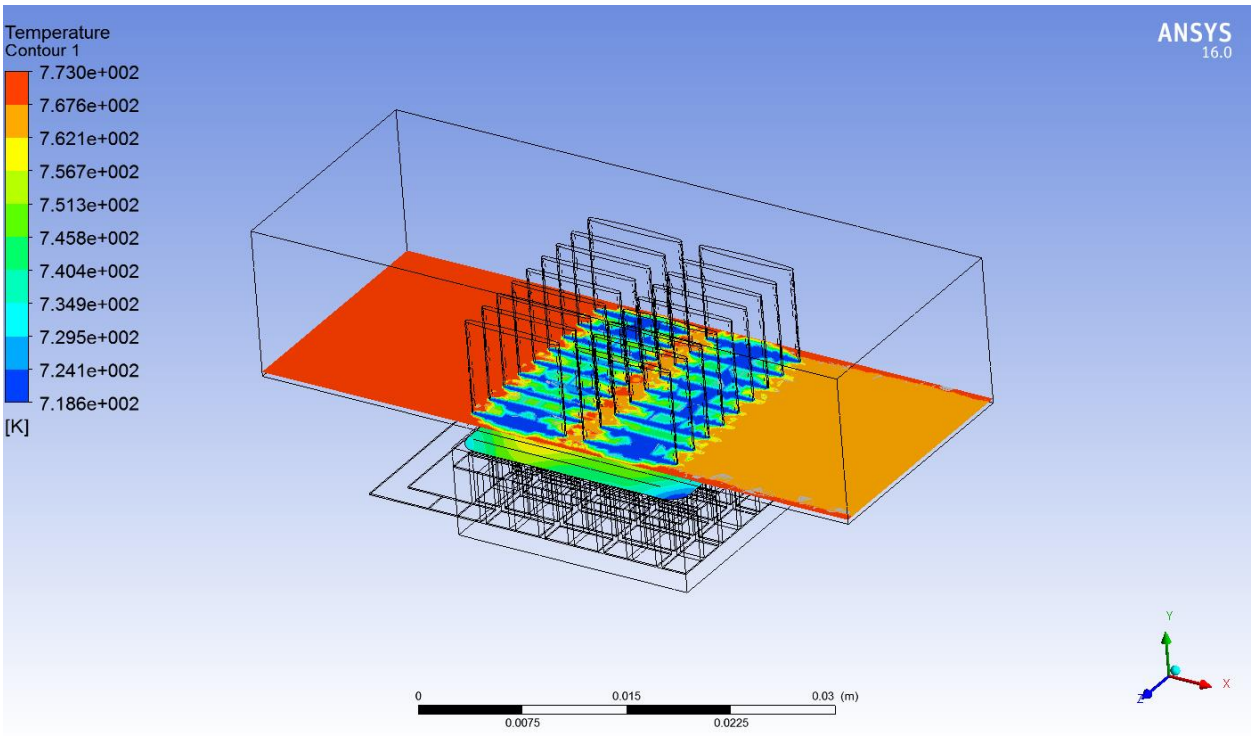

Figure 5-10 Temperature contour across the heat sink

This figure is obtained with inlet flow temperature $\mathbf{T_{in} = 773K}$, cold side ceramic temperature $\mathbf{T_c = 288K}$, mass flow rate $\boldsymbol{m_{dot}}$ **= 35 g/s** and air as the fluid.

Once the temperature gradient is formed in the heat sink and the heat transfer is analyzed, this set up and all the parameters are then linked to a thermal-electric module to solve for the thermoelectric equations. Using the ANSYS set up, the link can be defined as shown in the following figure.

Once the solution of the CFX is linked to this thermal- Electric module, coupling of physics is established and parameters like the temperatures are thus imported as shown in the following figure.

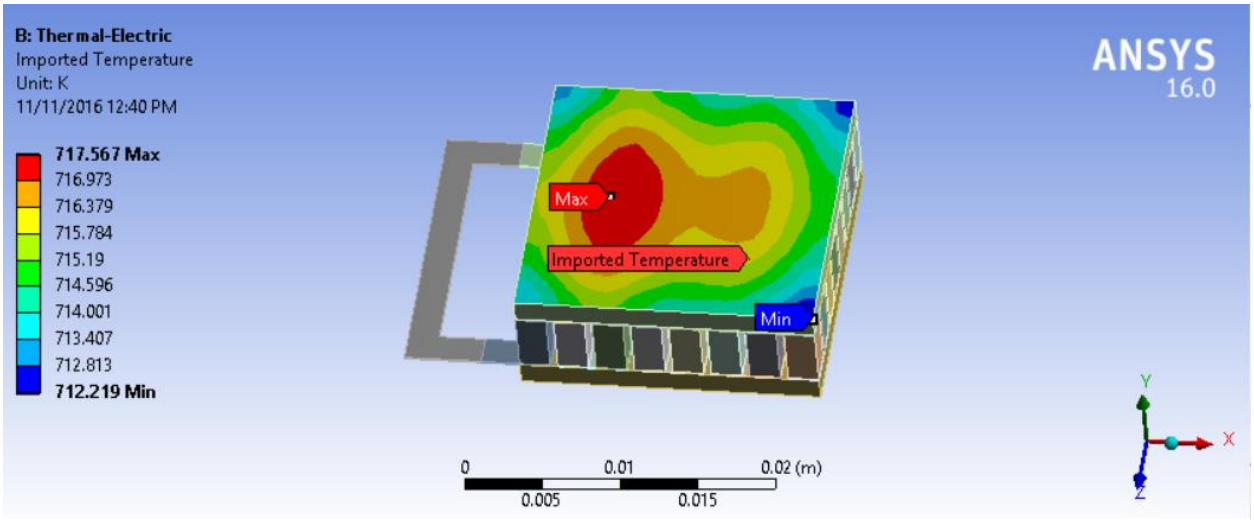

Figure 5-11 Imported temperature on the hot side

It has to be observed that the temperature imported on the surface is almost a constant and the color difference only implies that there is a minimum and a maximum temperature with a very small gradient.

5.3.3 Temperature gradient in the module

After the import, the module has to be solved for the thermoelectric effect. Inputs have to be given in the form of hot side temperature, cold side temperature and load resistance. The temperature gradient across the module is shown in the following figure.

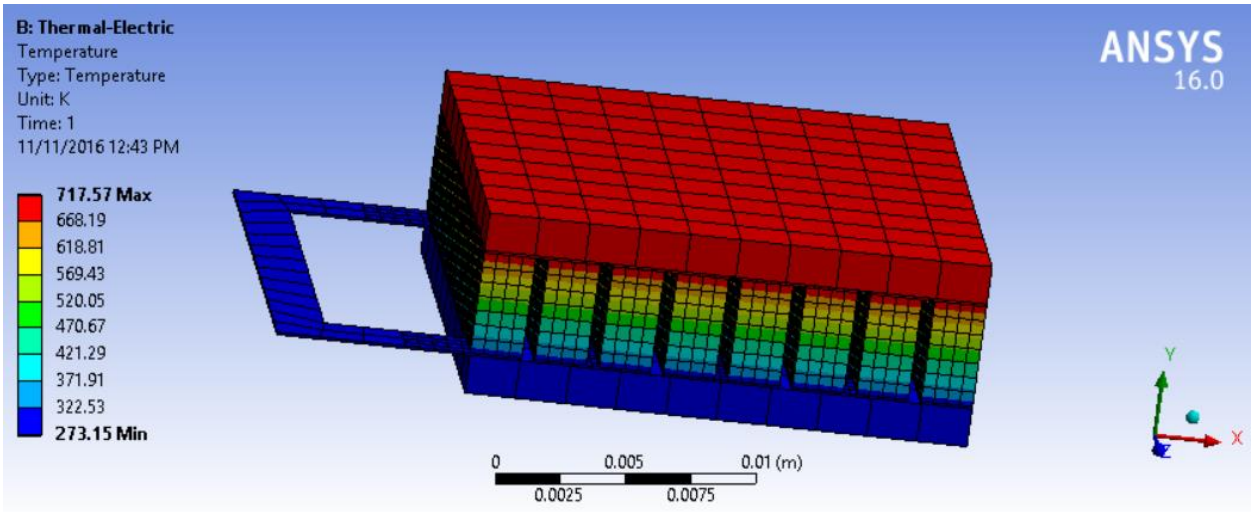

Figure 5-12 Temperature gradient along the module

This figure is obtained with inlet flow temperature $\mathbf{T_{in} = 773K}$, cold side ceramic temperature $\mathbf{T_c = 288K}$, mass flow rate $\boldsymbol{m_{dot}}$ **= 35 g/s** and air as the fluid.

5.3.4 Voltage output in the module

After the simulation of a thermoelectric generator module, the following result is obtained with respect to the potential difference in the module which leads to the generation of current.

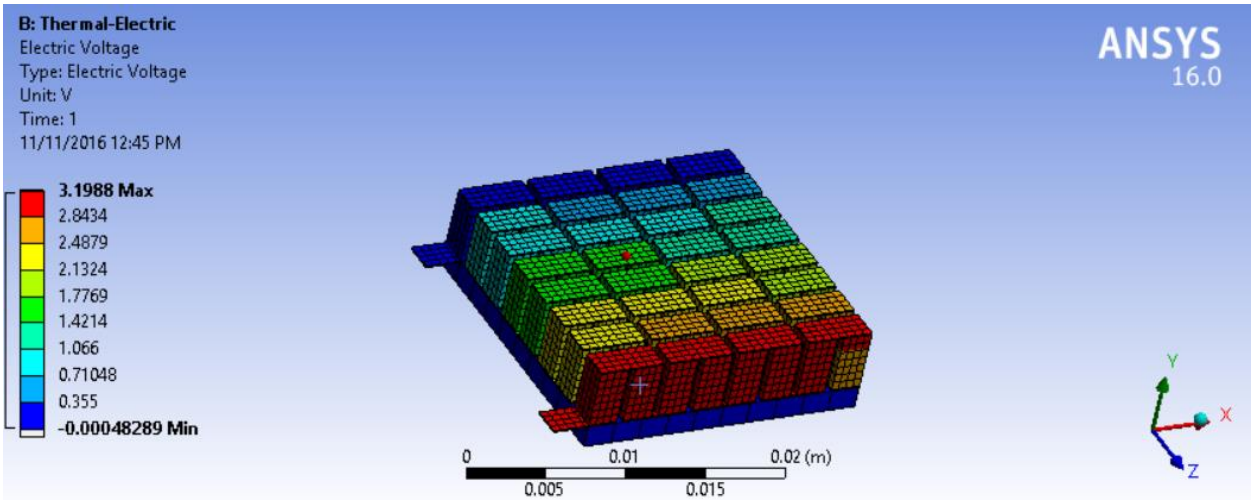

Figure 5-13 Voltage generated in the TEG module

This figure is obtained with inlet flow temperature $\mathbf{T_{in} = 773K}$, cold side ceramic temperature $\mathbf{T_c = 288K}$, mass flow rate $\boldsymbol{m_{dot}}$ **= 35 g/s** and air as the fluid.

All the results from this simulation are later validated with analytical modeling to see the accuracy of the simulation.

5.3.5 Power output vs leg length

After the import of the CFX model in ANSYS to the thermal electric model, results were obtained. A comparison of MathCad results with the simulated data was done. The figure below shows the power output at varying leg lengths and at resistance ratio unity. The results show the theoretical modeling and the numerical modeling and they are in very good agreement with each other.

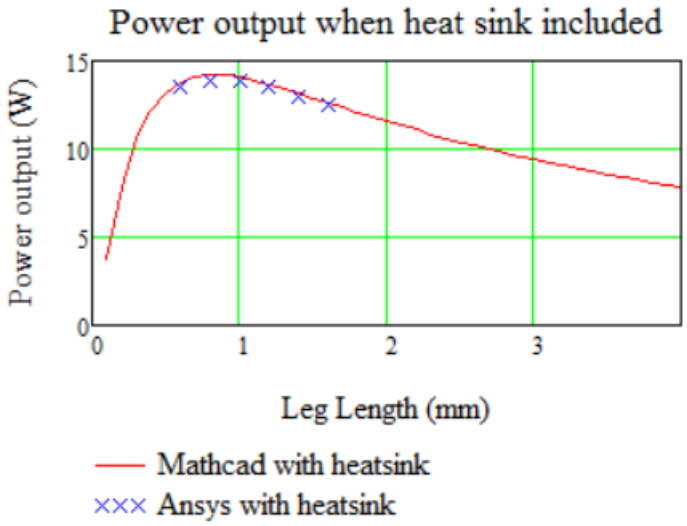

Figure 5-14 Power output vs leg length in the presence of a heatsink

This figure is obtained with inlet flow temperature $\mathbf{T_{in} = 773K}$, cold side ceramic temperature $\mathbf{T_c = 288K}$, mass flow rate $\boldsymbol{m_{dot}}$ **= 35 g/s** and air as the fluid. The load resistance is unity.

The convection conductance K_{conv} explained in section 4.3.2 was obtained to be 2.511 W/K. This convection conductance is in series with the conductance of the heat sink and hence the overall conductance decreases which decreases the power output. This can be seen when we compare the power output of the system with heat sink and without heat sink as shown in below.

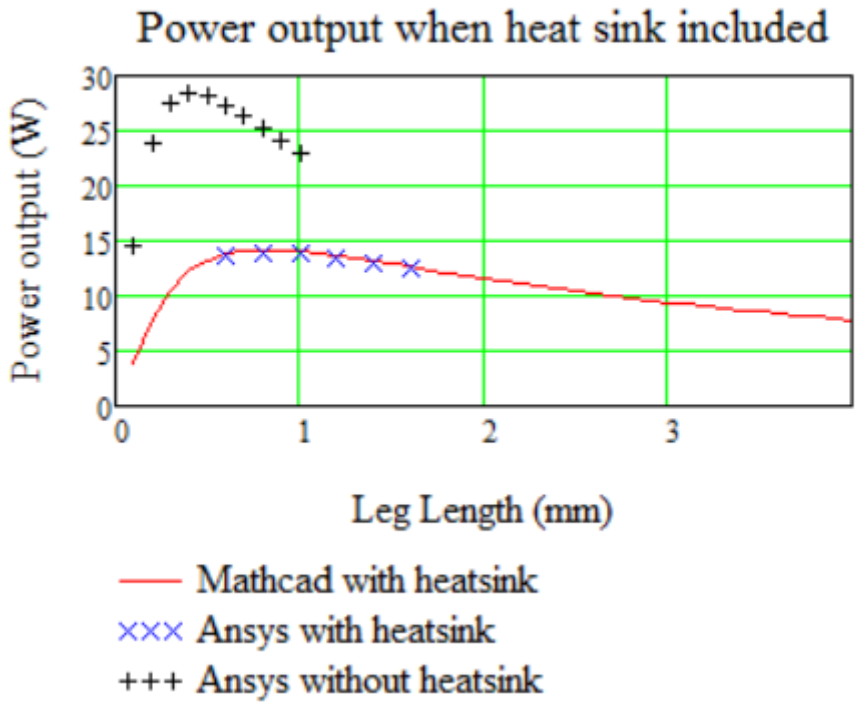

Figure 5-15 Comparison of power output with and without heatsink

This proves that the ANSYS simulation is a very good tool to predict the performance of a TEG. The above study can be extended to a TEG system which consists of a number of TE modules which increases the complexity of the problem. Problems with such high complexity can be easily solved using ANSYS.

6 CONCLUSION

Discussion has been made in detail based on the impact of electrical contact resistance and copper resistance at low leg lengths. It can be concluded that as the leg length reduces beyond 0.5mm, the value of these resistances are in comparison with the value of the leg length. Hence they cannot be ignored and also impact the power output and efficiency while analytically calculating these values. A comparison was made between the analytical model and the numerical model that were in good agreement with each other. It has to be noted that MathCad equations are a one dimensional set up while ANSYS simulation is a three dimensional set up. Since in this work, ANSYS model has been validated using the MathCad equations, it is safe to conclude that the analytical modeling in one dimension is sufficient to calculate the power output of a given thermoelectric module which is less complicated. Also, the isothermal plots shown conclude that the heat flow is in one dimensional. It can be noted that the power output has a significant increase in its value at low leg lengths when compared to higher leg lengths. It is however difficult to manufacture legs of this scale and hence ANSYS can be used as a tool and the system can be simulated to check the validity of the given equations before manufacturing the module. Based on these conclusions, modules can be chosen according to their applications and the manufacturer can chose the module accordingly.

7 FUTURE SCOPE

- This procedure can be used to extend the study to a complete system that includes more than one module and integrate it with a heatsink.
- Temperature dependent material properties can be included in this study in order to determine its impact on the overall power output of the module or system.
- More improvement can be done on this study with regards to the ceramic material used. One other potential material that can be used as a thermal contact material is diamond that has a very high thermal conductivity.

BIBLIOGRAPHY

[1] H. Lee, "The Thomson effect and the ideal equation on thermoelectric coolers," *Energy*, vol. 56, pp. 61-69, 2013.

[2] S. S. J. G. P.K.S. Nain, "Non-Dimensional Multi-Objective Performance OPtimization of Single Stage Themoelectric Cooler," *Springer,* pp. 404-413, 2010.

[3] X. M. S.B. Riaffat, "Thermoelectronics: a review of present and potential applications," *Applied Thermal Engineering* , vol. 23, pp. 913-935, 2003.

[4] D. Rowe, "Thermoelectics: an environmentally-friendly source of electric power," *Renewable energy*, vol. 16, pp. 1251-1256, 1999.

[5] T. Haruyama, "Performance of Peltier elements as a cryogenic heat flux sensor at temperature down to 60 K," *Cryogenics,* vol. 41, pp. 335-339, 2001.

[6] M. R. e. al., "Development of a thermoelectric sensor for ultrasonic intensity measurement," *Ultrasonics,* vol. 33, pp. 139-146, 1995.

[7] F. V. e. al, "Modelling of a microelectromechanical thermoelectric cooler, Sensors and Actuators," *A: Physical,* vol. 75, pp. 95-101, 1999.

[8] H. S. e. al., "A thermoelectric sensor for fluid flow measurement, principle, calibration and solution for self temeperature compensation," *Flow Measurement and Instrumentation,* vol. 9, pp. 135-141, 1998.

[9] A. Attar, "Studying the Optimum Design of Automotive Thermoelectric Air Conditioning," Kalamazoo, 2015.

[10] C. Vinning, "An inconvenient truth about thermoelectrics," *Nature Materials,* vol. 8, no. 2, pp. 83-85, 2009.

[11] J. L. T. a. J. H. C.W. Maranville, *Improving efficiency of a vehicle HVAC system with comfor modeling, zonal design, and thermoelectric devices,* 2012.

[12] H. Lee, "The Thomson Effect and the ideal equation on Thermoelectric Coolers," *Energy,* vol. 56, pp. 61-69, 2013.

[13] H. Lee, Thermal Design: Heat Sinks, Thermoelectrics, Heat Pipes, Compact Heat Exchangers, and Solar Cells, Hobooken: John Wiley & Sons, Inc., 2010.

[14] H. Lee, Thermal Design: Heat Sinks, Thermoelectrics, Heat Pipes, Compact Heat Exchangers, and Solar Cells, Hoboken: John Wiley & Sons, Inc., 2010.

[15] H. Lee, A. Attar and S. Weera, "Performance Prediction of Commercial Thermoelectric Cooler Modules using the Effective Material Properties," *Journal of Electronic Materials,* vol. 44, no. 6, pp. 2157-2165, 2015.

[16] D. C. a. M. K. J.R. Sootsman, *New and old concepts in thermoelectric materials,* 2009.

[17] N. Junior, "Modeling a thermoeelctric HVAC System for Automobiles," *Journal of Electronic Materials,* vol. 38, no. 7, pp. 1093-1097, 2009.

[18] H. Lee, "Optimal design of thermoelectric devices with dimensional analysis," *Applied Energy,* vol. 106, pp. 79-88, 2013.

[19] H. O. O. G. C. G. P. L. Y. Apertet, "Optimal working conditions for thermoelectric generators with realistic thermal coupling," *EPL,* vol. 97, 2012.

[20] D. M. R. a. G. Min, " Design theory of thermoelectric modules for electric power generation," *IEE Proc.-Sci. Meas. Technology,* vol. 143, pp. 351-356, 1996.

[21] G. E. S. U. V. K. G. D. O. a. W. W. Birkholz U., "Conversion of Waste Exhaust Heat in Automobile using FeSi2 Thermoelements," *7th International Conference on Thermoelectric Energy Conversion, Arlington,* pp. 124-128, 1988.

[22] C. R. J. a. E. N. B. Bass J., "Thermoelectric Generator Development for Heavy-Duty Truck Applications," *Annual Automotive Technology Development Contractors Coordination Meeting, Dearborn, Michigan,* pp. 743-748, 1992.

[23] E. N. B. a. L. F. A. Bass J. C., "Performance of the 1 kW thermoelectric generator for diesel engines," *AIP Conf. Proc.,* vol. 316(1), pp. 295-298, 1994.

[24] M. M. F. K. K. M. I. T. a. S. K. Ikoma K., "Thermoelectric module and generator for gasoline engine vehicles," *XVII International Conference on Thermoelectrics, IEEE,* pp. 464-467, 1998.

[25] H. B. a. K. M. A. Thacher E. F., "Progress in Thermoelectrical Energy Recovery from a Light Truck Exhaust," *Proc. DEER Conference, Detroit, Michigan,* 2006.

[26] H. B. T. K. M. A. a. R. C. J. Thacher E. F., "Testing of an automobile exhaust thermoelectric generator in a light truck," *Proc. Inst. Mech Eng. Part J. Automob. Eng,* vol. 221(1), pp. 95-107, 2007.

[27] H. Y. Y, "A mathematic model of thermoelectric module with applications on waste heat recovery from automobile engine," *Energy*, vol. 35(3), p. 1447–1454, 2010.

[28] H. Lee, Thermoelectrics- Design and Materials, John Wiley and Sons, 2016.

[29] [Online]. Available: http://homepages.wmich.edu/~leehs/ME539/TEG%20Tutorial.pdf.

[30] H. T. K. N. M. O. a. A. Y. XIAOKAI HU, "Three-Dimensional Finite-Element Simulation for a Thermoelectric Generator Module," *Journal of ELECTRONIC MATERIALS,* vol. 44, no. 10, 2015.

[31] T. o. discretization, *Ansys Help Viewer,* Release 2016.

[32] Ansys, *Thermoelectrics,* Release 16.

[33] Ansys, *CFX, Therory Guide,* 2016 Release.

[34] H. T. K. N. M. O. a. A. Y. XIAOKAI HU, "Three-Dimensional Finite-Element Simulation for a Theroelectric Generator Module," *Journal of ELECTRONIC MATERIALS,* vol. 44, p. 10, 2015.

[35] A. Attar, H. Lee and S. Weera, "Optimal Design of Automotive Thermoelectric Air Conditioner (TEAC)," *Journal of Electronic Materials,* vol. 43, no. 6, pp. 2179-2187, 2014.

[36] A. Attar, H. Lee and S. Weera, "Experimental Validation of the Optimum Design of an Automotive Air-to-Air Thermoelectric Air Conditioner (TEAC)," *Journal of Electronic Materials,* vol. 44, no. 6, pp. 2177-2185, 2015.

[37] A. Attar and H. Lee, "Designing and testing the optimum design of automotive air-to-air thermoelectric air conditioner (TEAC) system," *Journal of Electronic Materials,* no. Manuscript sumbitted for publication, 2015.

[38] [Online]. Available: https://www.alphanovatech.com/dxf/UB.pdf.